



OPEN Seasonal dynamics of thraustochytrids in mangrove rhizospheres for microbial interactions, PUFA production

Kalidasan Kaliyamoorthy^{1✉}, Kathiresan Kandasamy², Suchana Chavanich^{1,3}, Niyom Kamlangdee⁴, Nambali Valsalan Vinithkumar⁵ & Voranop Viyakarn^{3✉}

This study investigated seasonal variations of thraustochytrids in rhizosphere soil collected from two mangrove species *Rhizophora apiculata* and *Avicennia marina* in natural and planted mangrove stands. Thraustochytrid counts were higher in the natural mangrove stand than in the planted site. The counts varied seasonally, being highest in the post-monsoon season followed by summer, monsoon, and pre-monsoon. Thraustochytrid counts exhibited positive correlations ($p < 0.01$) with counts of Total heterotrophic bacteria (THB), azotobacters, actinobacteria, fungi, yeasts, and *Trichoderma*. However, a negative correlation was observed with cyanobacteria. The counts also had positive correlation with silt, clay, nitrogen, phosphorus, potassium, chromium, copper, magnesium, cadmium, zinc and redox potential, but, negative correlations with temperature, pH, pore water salinity, total organic carbon and sand content of the soil samples. In the present study, 113 thraustochytrid strains were isolated from mangrove habitats. However, only 48 pure cultures survived after being sub-cultured three times. Based on survivability, color, and shape, two isolates from each sampling site in each season were selected. The predominant 24 isolates were identified based on their morphological, and molecular characteristics and were classified under five genera: *Thraustochytrium*, *Schizochytrium*, *Botryochytrium*, *Parietichytrium*, and *Aurantiochytrium*. Among the isolates, *Aurantiochytrium* sp. (AKTSK-06) produced the highest biomass of 15.71 g/L in the post-monsoon season (January–March, 2023), and *Aurantiochytrium* sp. (PVTSK-03) accumulated the highest lipid content of 61.33%. Thraustochytrids were found to contain Omega-3 poly unsaturated fatty acids (PUFAs), such as EPA up to 8.89% in *Aurantiochytrium* sp. (VRTSK-01), DPA up to 9.65% in *Aurantiochytrium* sp. (AKTSK-03), and DHA up to 47.46% in *Aurantiochytrium* sp. (AKTSK-06). Thus, mangroves provide an ideal ecological niche for thraustochytrids with an abundant supply of omega-3 fatty acids for potential industrial applications.

Keywords Mangroves, Microbes, Thraustochytrids, Rhizosphere soil, Biomass, Lipids-Omega-3 fatty acids

Thraustochytrids are marine eukaryotic stramenopile protists, abundant in association with decomposing litter, sediments, and waters of mangrove biotopes^{1,2}. Thraustochytrids, along with other saprophytic microbes, play a vital role in decomposing organic matter in the mangrove habitat. This not only enriches the environment with nutrients but also converts litter into detritus food for fishes, making the mangrove habitats highly productive and operating the marine food chain^{3–5}. Thraustochytrids are extensively studied in estuarine, coastal, and mangrove habitats in various countries, including Chile⁶, China⁷, Sweden⁸, Malaysia⁹, Korea¹⁰, Thailand¹¹, Italy¹², Taiwan¹³, and Vietnam¹⁴. However, limited studies on thraustochytrids are available from Indian mangrove habitats in Mumbai⁵, Goa¹⁵, Kerala¹⁶, Tamil Nadu¹⁷, and Andaman¹⁸.

¹Center of Excellence for Marine Biotechnology, Department of Marine Science, Faculty of Science, Chulalongkorn University, Bangkok, Thailand. ²Faculty of Marine Sciences, Annamalai University, Parangipettai 608 502, India. ³Aquatic Resources Research Institute, Chulalongkorn University, Bangkok, Thailand. ⁴Department of Microbiology, Faculty of Science, King Mongkut's University of Technology, Thung Khru, Thonburi, Bangkok 10140, Thailand. ⁵Deep Ocean Mission Vertical 6, Advanced Marine Station for Ocean Biology, National Institute of Ocean Technology, Pallikaranai, Chennai, Tamil Nadu 600 100, India. ✉email: marinedasan87@gmail.com; Voranop.V@chula.ac.th

Thraustochytrids are known for their fast cell growth rate, and high production of lipids and fatty acids, including myristic acid, and palmitic acid, which are potentially useful as a sustainable feed stock and in the biodiesel sector^{5,19}. They are rich in Omega-3 polyunsaturated fatty acids (PUFAs), particularly docosahexaenoic acid (DHA), which is essential for the brain, retina, new tissue formation, foetal neural development, and visual sensory development in humans and fish larvae^{20,21}. DHA is primarily derived from fish or fish oils. However, it is important to note that fish oil contains relatively low levels of DHA¹⁸. Depletion of fish stock and bioaccumulation of toxins such as polychlorinated biphenyls (PCBs), dioxins, and toxic heavy metals in fish pose a serious threat, preventing the fulfilment of the growing need for DHA in the market⁵. Thraustochytrids have the potential to overcome these challenges by serving as an alternative source for producing toxin-free PUFAs through bioprocess technology. However, there is limited work on seasonal changes in the biomass production, lipid content and fatty acid composition of thraustochytrids. These studies are largely available for natural mangrove stands but not for planted mangrove habitats. To address the gaps in knowledge, the present work was undertaken to understand spatial and temporal variations in thraustochytrids isolated from root-soil samples of two mangrove species (*Rhizophora apiculata* and *Avicennia marina*) in natural or restored mangrove areas for microbial counts, biomass, lipid content, fatty acid composition, influenced by the physicochemical conditions of mangrove soils.

Materials and methods

Study area

Soil samples were collected around the roots of two predominant mangrove namely, *Avicennia marina* (Forsk.) Vierh, and *Rhizophora apiculata* Blume, from one natural mangrove forest site and two planted sites, along the Bay of Bengal on the southeast coast of India. The former site is located at Lat. 11° 42' 45.59 N; Long. 79° 79' 51.87 E in Pichavaram, and the latter two sites are located at Lat. 11° 54' N; Long. 79° 50' E in Ariyankuppam estuary and at Lat. 11° 29' N; Long. 79° 47' E in Vellar estuary (Fig. 1). The study area map was developed using ArcMap software, version 10.8 (Esri, Redlands, California, U.S.). The Vellar river, originating from the Servarayan hills and flowing 480 km to the Bay of Bengal, features 15–20-year-old mangrove vegetation. This estuary connects to Pichavaram via a backwater channel, which is blocked by a sandbar in summer. Pichavaram is an estuarine mangrove habitat with 51 islets ranging from 10 m² to 2 km², linked by intricate waterways. It is influenced by neritic, brackish, and fresh waters, covering approximately 1100 ha. It covers approximately 1100 ha, with

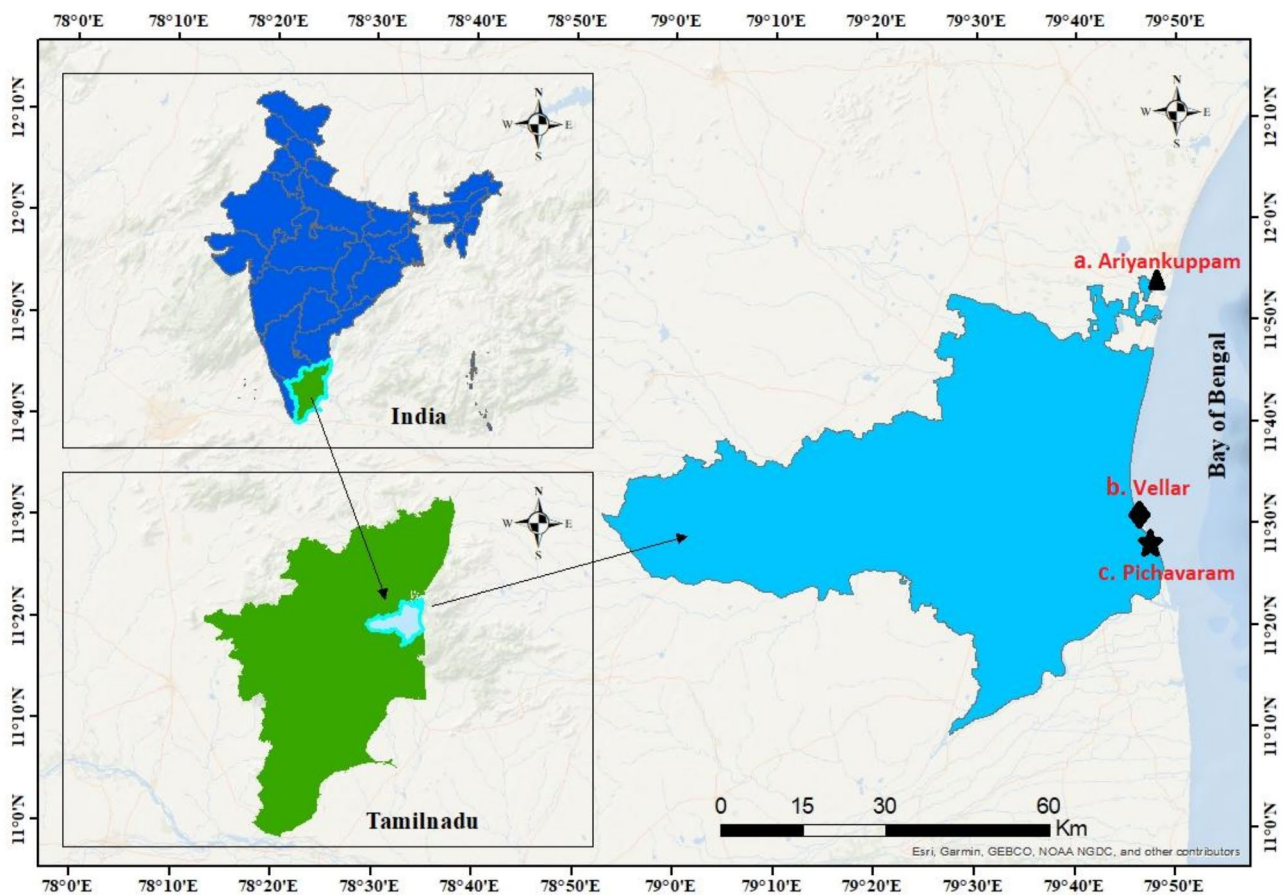


Fig. 1. Study area, located along the Bay of Bengal on the southeast coast of India (a. Ariyankuppam Estuary (Planted) b. Vellar Estuary (Planted) and c. Pichavaram (natural mangrove forest)).

50% forest, 40% waterways, and the remainder sand and mud-flats. Tides are semi-diurnal, varying from 15 to 100 cm, with depths ranging from 0.3 to 3 m. Ariyankuppam estuary, in southern Pondicherry, is seasonally bar-built and flows eastward into the Bay of Bengal, features 15- 18-year-old mangroves. The estuary benefits from agricultural, industrial, and municipal waste, contributing to its lush vegetation. All the three sampling sites were rise and fall of the tidal waters is through a direct connection with the sea at a river mouth and also through the two adjacent estuaries.

Seasonal soil sample collection, physio-chemical parameters, texture, nutrient analysis

Surface soil samples (0–10 cm) were collected manually around the mangrove roots using a 1.5 m long, 50 cm diameter stainless-steel corer during low tide, when the substrate was completely exposed, from three sampling sites. At each site, 100 g of mangrove root-associated soil was collected at 1–5 m intervals, with the same mangrove species sampled at each location. The sampling was conducted in all four seasons: pre-monsoon (July–September 2022), monsoon (October–December 2022), post-monsoon (January–March 2023), and summer (April–June 2023). Triplicate samples were collected during each season. The soil samples were analysed in-situ for temperature, pH, pore-water salinity (‰), and redox potential (Eh). A hand refractometer (Erma INC, Tokyo) was used to test salinity, a millivoltmeter (Wissenschaftlich-Technische Werkstätten, Germany) were used to measure pH and redox potential (Eh), and a thermometer was used to measure temperature with an precision of 0.5 °C. Additionally, the samples were analysed for the percentage composition of sand, silt, and clay particles using a sieve shaker, as well as the total organic carbon content²². The soil samples were dried in an oven at 110 °C until they reached a constant weight. After that, they were ground into a fine powder and analyzed for their total carbon content, and C/N ratio using a CHN/O analyzer (Perkin Elmer-series II 2400). The soil samples were analyzed for nitrogen (N), and phosphorus (P)²³, and potassium (K)²⁴. The soil samples were also analysed for metal content using an inductively coupled plasma emission spectrometer (JOBIN YVON–JY 24, France) for zinc (Zn), magnesium (Mn), copper (Cu), cadmium (Cd) and chromium (Cr) with the help of the calibration curves²⁵. All media components, chemicals, and analytical reagents were obtained from Hi-Media, BioScience (Mumbai, India).

Soil microbiological analysis

Soil samples were collected in sterile zip-lock bags, and immediately transported to the laboratory, where they were kept at 4 °C. They were then examined for microbial counts within 4–6 h of collection. One gram of soil was transferred aseptically to a sterile conical flask containing 99 ml of sterile natural seawater (30 ppt). This mixture was mechanically shaken for approximately 5–10 min before being serially diluted up to 10^{–5} with sterilized natural seawater. The dilutions were then plated on specified culture medium using the spread plate method to enumerate various microbial counts: Total heterotrophic bacteria (THB) were cultured on Zobell marine agar (ZMA)²⁶, cyanobacteria on salt nutrient media (SNM)²⁷, lactobacillus on deMan rogosa and Sharpe agar (MRSA)²⁸, actinobacteria on actinobacteria isolation agar (AIM)²⁹, azotobacters on Winogradsky agar (WA)³⁰, yeasts on yeast malt agar (YMA)³¹, *Trichoderma* on *Trichoderma* selective agar (TSA)³², fungi on potato dextrose agar (PDA)³³ and glucose yeast peptone agar (GYPA) medium was used for Thraustochytrids¹⁸. All these culture media were prepared in 30 ppt natural seawater with the addition of nutrient components, along with antifungal and antibacterial agents (Hi-Media, India) to prevent contaminations during the isolation process without affecting the microbial growth. The antibiotics and their concentrations used were as follows: for heterotrophic bacteria (fluconazole 100 µg L^{–1} and nystatin 50 µg L^{–1}); Actinobacteria (fluconazole 100 µg L^{–1} and nalidixic acid 25 µg mL^{–1}); Lactobacilli (fluconazole 100 µg L^{–1} and nalidixic acid 25 µg mL^{–1}); Azotobacters (fluconazole 100 µg L^{–1} and erythromycin 100 µg L^{–1}); Cyanobacteria (fluconazole 100 µg L^{–1} and erythromycin 100 µg L^{–1}); fungi (streptomycin 100 µg L^{–1} and ampicillin 100 µg L^{–1}); yeasts (streptomycin 100 µg L^{–1} and ampicillin 100 µg L^{–1}); *Trichoderma* (streptomycin 100 µg L^{–1} and ampicillin 100 µg L^{–1}); and Thraustochytrids (streptomycin 100 µg L^{–1} and fluconazole 150 µg L^{–1}). These agents were selected to inhibit unwanted microorganisms while allowing the growth of the target species. During microbial isolation, the culture plates were incubated in an incubator set to the temperature of the sampling site. Samples were collected across different seasons, and the pure colonies were subsequently maintained at 28 ± 2 °C. All determinations were performed in triplicates. Microbial colonies were counted after incubation periods of 2–3 weeks for cyanobacteria; 7–10 days for *Trichoderma*, actinobacteria, azotobacters, and lactobacilli; 2–7 days for yeasts, and thraustochytrids; and, 2–3 days for THB. The microbial colony forming unit (CFU) was calculated and then expressed as CFU per gram of soil.

Morphological and molecular identification of thraustochytrids

Thraustochytrid isolates/colonies were identified based on their morphological characteristic, including color, shape, and margin of colonies, cellular structures, ecoto-plasmic network, binary divisions, cluster formation, amoeboid cells, and zoospore production, as observed under a light microscope (Olympus, Japan) at 40× and 100× magnifications³⁴. The culture plates were examined daily to monitor the growth, development, and presence of any contamination of colonies. After 3–4 subcultures, the pure axenic colonies from the mother cultures were preserved in 20% (v/v) glycerol stocks at –80 °C for further use. The molecular identification of thraustochytrids was carried out using a modified version of the method described by Kalidasan et al. (2023)³⁵. Initially, 5 mL of a 48-hour-old cell culture was centrifuged at 8,000 × g for 10 min at 4 °C. The pellet was resuspended in 200 µl of lysis buffer (0.1 M EDTA, 0.25 M Tris-HCl, pH 8.2), 0.1 M NaCl, and 2% sodium dodecyl sulfate, and then incubated in a water bath at 55 °C for 65 min for homogenization. DNA was extracted using chloroform-isoamyl alcohol and precipitated with chilled isopropanol. The purified DNA was dissolved in 30 µl of TE buffer and stored at –20 °C until further use. Gene amplification was performed using primers 18S001 (5′-AACCTGGTTGATCCTGCCAGTA-3′) and 18S13 (5′-CCTTGTTACGACTTCACCTTCCTCT-3′). A molecular weight marker (100 bp ladder) was used to determine the size of the amplicons. The PCR products

were analyzed by electrophoresis on a 1.2% agarose gel and visualized with ethidium bromide staining. PCR product purification and DNA sequencing were performed using the MegaBace high-output sequencer (Yaazh Xenomics, Coimbatore, India). The raw sequences obtained were processed using MEGA 6.0 software (Mega Version 6, Pennsylvania, USA), with unreliable peaks excluded from analysis. The amplified 18 S rDNA gene sequences were compared against reference sequences using the BLAST program on the NCBI website, with a similarity threshold of 95–100% indicating species identification. All sequences were submitted to GenBank via Bankit following NCBI procedures. The thraustochytrid rDNA sequences were successfully sequenced, aligned, and analyzed using the CLUSTAL W Multiple Sequence Alignment Program.

Biomass production and determination of dry cell weight

The pure colonies of thraustochytrids isolates were cultured individually in a medium comprising glucose (5 g L⁻¹), peptone (1.25 g L⁻¹), yeast extract (1.25 g L⁻¹), agar (12 g L⁻¹) in natural seawater with the addition of antibacterial (streptomycin 100 µg L⁻¹), and antifungal (fluconazole 150 µg L⁻¹) agents to prevent contamination. In order to conduct further studies, two isolates were selected from each season, resulting in a total of 24 predominant isolates were chosen based on better survival, and high growth rates. The selected isolates were cultured in basal media prepared in a sterile 1000 mL natural seawater production broth medium containing glucose (10 g L⁻¹), yeast (1.25 g L⁻¹), peptone (3 g L⁻¹), and monosodium glutamate (1.25 g L⁻¹), in an Orbitek shaker at 150 rpm (SciGenics Biotech, Tamil Nadu, India), covered with a sterile cotton plug and aluminium foil to avoid light exposure¹⁸. Biomass production was conducted in culture flasks under controlled environmental conditions to determine the lipid and fatty acid content of thraustochytrids. The conditions in the culture flasks were set to match the environmental parameters from which samples were collected during different seasons such as Pre-monsoon: Salinity at 26.16 ± 1.13, pH at 7.65 ± 0.35, and temperature at 25.43 ± 1.10 °C. Monsoon: Salinity at 24.60 ± 1.20, pH at 7.34 ± 0.13, and temperature at 23.96 ± 1.20 °C. Post-monsoon: Salinity at 28.53 ± 1.66, pH at 7.65 ± 0.28, and temperature at 25.68 ± 1.50 °C. Summer: Salinity at 31.64 ± 1.55, pH at 7.87 ± 0.24, and temperature at 27.90 ± 0.73 °C. After 7 days of incubation, biomass was collected by centrifugation in a conical bottom centrifuge tube (50 mL) at 8000 × g for 10 min. To remove any remaining medium component, the cell pellet was washed thrice using sterile distilled water. The cell pellet was washed three times with sterile distilled water to eliminate any residual medium components. Afterward, the cell pellet samples were freeze-dried at -49 °C for 2 days to determine the biomass per liter in grams of dry weight. The resulting biomass was stored in airtight containers at -80 °C for future analysis.

Total lipid and fatty acid analysis

A 200 mg aliquot of lyophilized biomass cells was extracted for total lipids using a 2:1 ratio of chloroform and methanol³⁶. The extracted lipids were transferred to an air-tight vial and dried using nitrogen gas to remove the solvent. The dried lipid was then mixed with 1 ml of 3% methanolic hydrochloric acid, and incubated at 60 °C for 18 h to undergo trans-esterification³⁷. The upper organic phase was carefully transferred to a chromatographic vial and then evaporated using nitrogen gas until dry. Afterwards, 1 ml of ethyl acetate was added to the vial and the content was then analyzed for fatty acid methyl esters (FAME) using GC-MS (Agilent 7890 A – 240). The GC-MS was equipped with a silica capillary column (Agilent J&W, HP-5ms; Agilent Technologies). Helium was used as the carrier gas, flowing at a rate of 1 ml/min, with nitrogen serving as the mobile phase at a flow rate of 35 ml/min. The oven-temperature was programmed to start initially at 140 °C for 1 min, then increased at a rate of 2 °C/min until reaching the final temperature of 220 °C, which was held for 1 min. The injector temperature was set at 260 °C and 1 µl of the sample was injected with a split ratio of 100:1. An external standard mix (FAME Mix C4 - C24, Sigma Aldrich) was used to standardize the composition of fatty acid methyl esters in the sample. The FAME compounds were identified using the built-in NIST library software.

Statistical analysis

The data was analysed by using IBM-SPSS 16.0. Three-way ANOVA, Duncan multiple range test and Pearson's correlation were evaluated to compare the thraustochytrids in between soil sites, seasons, and mangrove species.

Results and discussion

Thraustochytrids and other microbial counts

The present work focuses on thraustochytrids on the southeast coast of India along with THB, lactobacillus, actinobacteria, azotobacter, fungi, *Trichoderma*, yeasts, and thraustochytrids, influenced by two mangrove species across three sampling sites for four different seasons. The results are presented in Table 1; Fig. 2. Thraustochytrid count were higher in the natural mangroves at Pichavaram (4.58×10^3 CFU/g) than in the planted mangrove sites at Ariyankuppam (4.15×10^3 CFU/g), and Vellar (3.95×10^3 CFU/g) (Table 1; Fig. 2a). The count was highest (4.26×10^3 CFU/g) in *R. apiculata* and lowest (4.20×10^3 CFU/g) in *A. marina* (Table 1; Fig. 2b). The count varied seasonally, with the highest count in the post-monsoon season (5.40×10^3 CFU/g), followed by summer (4.91×10^3 CFU/g), monsoon (3.43×10^3 CFU/g), and pre-monsoon (3.17×10^3 CFU/g) (Table 1; Fig. 2c). Thraustochytrid count showed statistically significant differences ($p < 0.01$) between sites or seasons, but not between mangrove species (Table 1). In our study, we observed notable differences in bacterial counts between *A. marina* (4.20×10^3 CFU/g) and *R. apiculata* (4.26×10^3 CFU/g). These differences can be attributed to various factors, including the distinct root structures, leaf litter composition, and the specific microhabitats created by these mangrove species. *A. marina*, known for its pneumatophores, provides a more oxygenated environment in the rhizosphere, which may support a different bacterial community composition compared to *R. apiculata*, which has prop roots that contribute to a different soil and nutrient dynamic. The differences in organic matter, nutrient availability, and root exudates (sugars, amino acids and phenolics) between the habitats of these two species likely influence the types and quantities of bacteria present. This allelopathic effect is already

Source	Microbial counts (CFU $\times 10^3$ g ⁻¹ of soil)								
	Cyanobacteria	THB	Lactobacillus	Azotobacter	Actinobacteria	Fungi	Yeasts	Trichoderma	Thraustochytrids
Mangrove site									
Vellar	1.05 \pm 0.1	17.82 \pm 5.38	4.87 \pm 1.47	4.44 \pm 0.82	5.32 \pm 1.46	6.13 \pm 1.74	3.56 \pm 0.88	3.95 \pm 1.12	3.95 \pm 0.99
Pichavaram	1.13 \pm 0.1	18.82 \pm 5.68	4.89 \pm 1.50	3.25 \pm 0.92	5.54 \pm 2.00	6.57 \pm 2.08	3.89 \pm 0.89	4.74 \pm 1.52	4.58 \pm 1.45
Ariyankuppam	1.33 \pm 0.4	18.12 \pm 7.04	3.66 \pm 1.12	2.92 \pm 0.87	4.98 \pm 1.42	6.08 \pm 2.18	2.84 \pm 0.93	4.51 \pm 1.19	4.15 \pm 1.02
Mangrove species									
<i>R. apiculata</i>	1.20 \pm 0.29	18.29 \pm 6.03	4.50 \pm 1.48	3.57 \pm 1.09	5.31 \pm 1.65	6.29 \pm 2.01	3.46 \pm 1.00	4.44 \pm 1.29	4.26 \pm 1.20
<i>A. marina</i>	1.14 \pm 0.29	18.21 \pm 6.06	4.44 \pm 1.48	3.51 \pm 1.09	5.25 \pm 1.65	6.23 \pm 2.01	3.40 \pm 1.00	4.74 \pm 1.52	4.20 \pm 1.19
Season of analysis									
Pre-monsoon	0.81 \pm 0.1	13.23 \pm 1.97	4.05 \pm 0.98	2.66 \pm 0.70	3.31 \pm 0.54	3.71 \pm 0.40	2.37 \pm 0.6	3.79 \pm 0.89	3.17 \pm 0.62
Monsoon	1.04 \pm 0.3	24.79 \pm 2.55	3.72 \pm 1.62	3.71 \pm 1.16	6.57 \pm 1.61	7.21 \pm 2.03	4.48 \pm 0.79	3.13 \pm 1.10	3.43 \pm 0.65
Post-monsoon	1.56 \pm 0.3	22.00 \pm 3.28	6.03 \pm 0.86	3.32 \pm 0.70	6.34 \pm 0.84	7.89 \pm 0.83	3.77 \pm 0.52	5.31 \pm 0.45	5.40 \pm 0.88 ^c
Summer	2.45 \pm 0.1	13.00 \pm 3.67	4.07 \pm 1.08	3.19 \pm 1.03	4.90 \pm 0.71	6.24 \pm 1.02	3.10 \pm 0.46	5.41 \pm 0.80 ^a	4.91 \pm 0.70 ^b
Site	**	**	**	**	**	NS	**	NS	**
Species	NS	NS	NS	NS	NS	NS	NS	NS	NS
Season	**	**	**	**	**	**	**	NS	**

Table 1. Microbial counts in soil samples of two mangrove species from three different sites under four seasons in the year 2022–2023. Values not sharing a common superscript differ significantly at $p > 0.05$; ** = $p < 0.01$; * = $p < 0.05$; NS = Not Significant.

found in our laboratory³⁸. Natural mangrove forest supported higher thraustochytrids counts (4.58×10^3 CFU/g) compared to planted mangroves. This spatial variation can be attributed to soil conditions, especially texture, composition, solar radiation, and organic matter of the sites³⁹. Thraustochytrid count exhibited a high positive correlation ($p < 0.01$) with the counts of other microbial groups - THB, azotobacter, actinobacteria, fungi, yeasts, lactobacillus, and *Trichoderma* - but, a negative correlation with cyanobacterial count (Table 1; Fig. 3). This supports the idea that saprophytic microbes with similar activities in decomposing organic matter colonize synergistically, while cyanobacteria, as autotrophs, behave differently from other saprophytes^{4,39}.

The THB count was higher in the natural mangroves at Pichavaram (18.82×10^3 CFU/g) than in the planted mangroves at Ariyankuppam (18.12×10^3 CFU/g), and Vellar (17.82×10^3 CFU/g) (Table 1). The THB count was high in *R. apiculata* (18.29×10^3 CFU/g) followed by *A. marina* (18.21×10^3 CFU/g) (Table 1). The THB count varied seasonally, with the highest in the monsoon (24.79×10^3 CFU/g) followed by post-monsoon (22.00×10^3 CFU/g), pre-monsoon (13.23×10^3 CFU/g), and summer (13.00×10^3 CFU/g) (Table 1). The THB count was found to be statistically significant ($p < 0.01$) between sites or seasons, but not between mangrove species. Mangroves are detritus-based ecosystems, that support a diverse population of saprophytic microorganisms that facilitate litter decomposition. Fungi are the major colonizers in mangrove habitat, generally peaking during the early stages of litter decomposition. After fungal colonization in the mangrove litter, bacteria grow rapidly to reach high densities, three times that of filamentous fungi^{40,41}. The THB count is generally higher than other microbial flora in the mangrove biotope. This is due to the litter decomposition process, which releases nutrients and helps in the multiplication of microorganisms in the mangrove soil⁴. The present study also recorded significantly higher total heterotrophic microbial counts ($18.82 \pm 5.68 \times 10^3$ CFU/g) in the natural mangrove soil than in the planted mangrove soil ($17.82 \pm 5.38 \times 10^3$ CFU/g). Moreover, the natural mangrove forest accumulates a greater amount of nutrients and undergoes remineralization through microbial processes, which further increases the microbial counts. As a result, natural mangrove habitats have higher microbial counts of lactobacillus, actinobacteria, azotobacter, fungi, yeasts and thraustochytrids than planted mangrove habitats. However, the counts of cyanobacteria, and azotobacter were recorded maximum in planted mangroves than in natural mangroves.

Cyanobacterial count was found to be higher in the planted mangroves at Ariyankuppam (1.33×10^3 CFU/g) than in the natural mangroves at Pichavaram (1.13×10^3 CFU/g), and Vellar (1.05×10^3 CFU/g) (Table 1). The count was highest in *R. apiculata* (1.20×10^3 CFU/g) followed by *A. marina* (1.14×10^3 CFU/g) (Table 1). The count varied seasonally, with the highest count in summer (2.45×10^3 CFU/g) followed by post-monsoon (1.56×10^3 CFU/g), monsoon (1.04×10^3 CFU/g), and pre-monsoon (0.81×10^3 CFU/g) (Table 1). Cyanobacterial count was found to be statistically significant ($p < 0.01$) between sites or seasons, but not between mangrove species. Cyanobacteria are an essential component of the microbiota in mangrove ecosystems providing an oxygen-rich and phosphorus-storing environment, contributing to carbon and nitrogen fixation, and facilitating resilience to extreme environmental stressors⁴². In the present study, the cyanobacterial count was high in the Ariyankuppam mangrove site ($1.33 \pm 0.4 \times 10^3$ CFU/g) during summer, consistent with a previous report⁴³.

Lactobacillus count was found to be high in the natural mangroves at Pichavaram (4.89×10^3 CFU/g) compared to the planted mangroves at Vellar (4.87×10^3 CFU/g), and Ariyankuppam (3.66×10^3 CFU/g) (Table 1). The count was higher in *R. apiculata* (4.50×10^3 CFU/g) followed by *A. marina* (4.44×10^3 CFU/g) (Table 1). The Lactobacillus count varied seasonally, with the highest count in the post-monsoon (6.03×10^3 CFU/g) followed by summer (4.07×10^3 CFU/g), pre-monsoon (4.05×10^3 CFU/g), and monsoon (3.72×10^3 CFU/g) (Table 1). The Lactobacillus count was found to be significant between sites or seasons ($p < 0.01$), but not

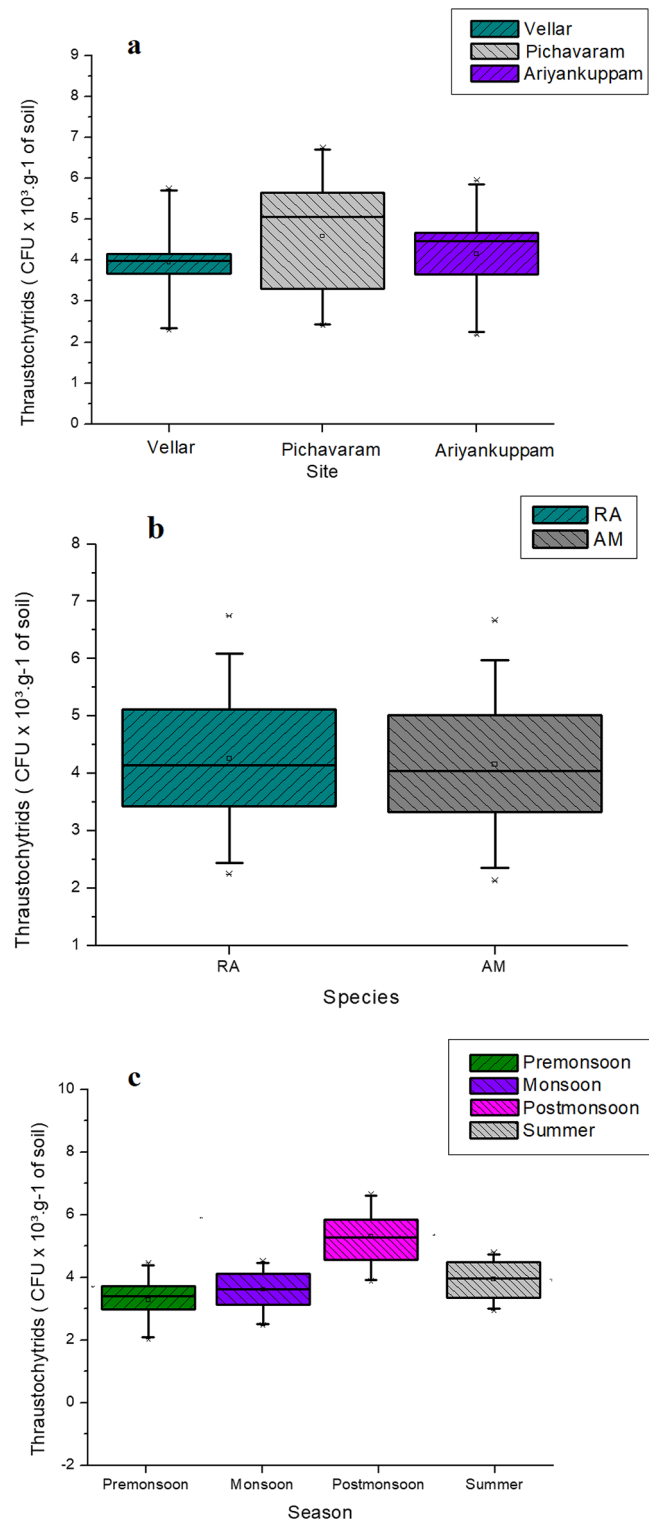


Fig. 2. Thraustochytrids count in relation to (a) Sites (b) Species (c) Seasons.

between mangrove species. Lactobacilli are gram-positive and non-spore forming cocci. They are highly diverse and productive, occurring in large quantities in soil especially around roots, utilizing plant-root exudates⁴⁴. Lactic acid bacteria were always higher in mangrove environment compared to other ecosystem. In a recent study, a total of 386 isolates of lactic acid bacteria were reported, collected from soil, water, leaves, twigs, and fruit in mangrove forests of southern Thailand⁴⁵. Similarly, the bacterial flora of mangrove litter fall and underlying sediments from South Andaman was investigated. Thirty-eight bacterial isolates were obtained from *Rhizophora*, *Avicennia*, and *Nypa* species. Cultural, morphological, and biochemical analyses revealed that most

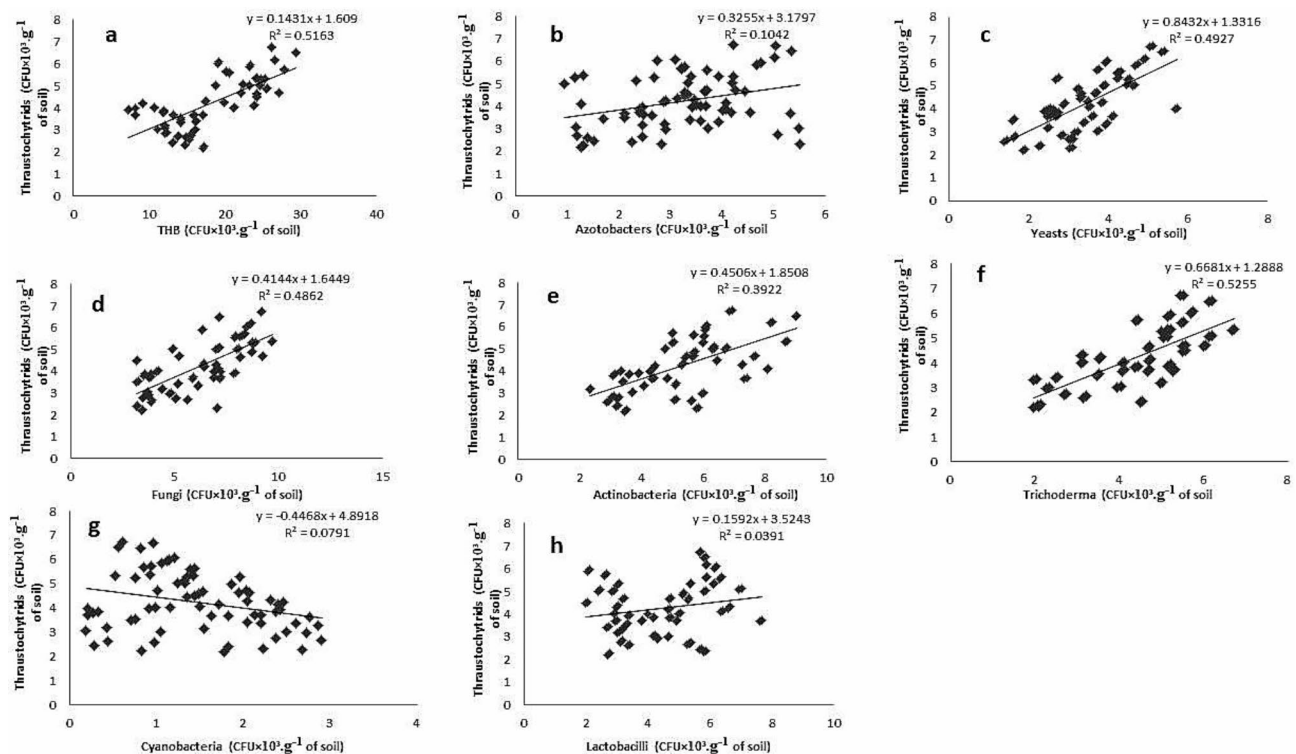


Fig. 3. Correlation between thraustochytrids count and other microbial group in mangrove soil.

isolates belonged to *Bacillus* spp. (50%). Specifically, 20 isolates came from *Rhizophora*, 13 from *Avicennia*, and 5 from *Nypa*-dominated areas. This indicates that *Rhizophora* sp. has higher microbial diversity, likely due to its greater annual litter fall compared to *Avicennia* sp., which promotes increased microbial degradation and a more productive mangrove environment⁴⁶. The current study observed high counts during the post-monsoon in the Pichavaram natural mangrove forest ($4.89 \pm 1.50 \times 10^3$ CFU/g) compared to the planted mangrove sites, similar to our earlier study⁴⁴.

Azotobacter count was higher in the planted mangroves at Vellar (4.44×10^3 CFU/g) than in the natural mangroves at Pichavaram (3.25×10^3 CFU/g), and Ariyankuppam (2.92×10^3 CFU/g) (Table 1). The count was maximum in *R. apiculata* (3.57×10^3 CFU/g) followed by *A. marina* (3.51×10^3 CFU/g) (Table 1). The count varied seasonally, with the highest count in the monsoon (3.71×10^3 CFU/g), followed by post-monsoon (3.32×10^3 CFU/g), summer (3.19×10^3 CFU/g), and pre-monsoon (2.66×10^3 CFU/g) (Table 1). Azotobacter count was found to be significant ($p < 0.01$) between sites or seasons, but not between mangrove species. Azotobacter plays a vital role in nitrogen fixation by facilitating nutrient remineralization, providing essential nutrients to plants, and ultimately increasing plant growth⁴⁷. The present work observed high count of Azotobacter in the monsoon ($3.71 \pm 1.16 \times 10^3$ CFU/g), in contrast to our earlier report that recorded high count in the post-monsoon⁴⁸.

Actinobacterial count was found to be high in the natural mangroves at Pichavaram (5.54×10^3 CFU/g) compared to that in the planted mangroves at Vellar (5.32×10^3 CFU/g), and Ariyankuppam (4.98×10^3 CFU/g) (Table 1). The count was higher in *R. apiculata* (5.31×10^3 CFU/g) followed by *A. marina* (5.25×10^3 CFU/g) (Table 1). The count varied seasonally, with the highest count in the monsoon (6.57×10^3 CFU/g), followed by post-monsoon (6.34×10^3 CFU/g), summer (4.90×10^3 CFU/g), and pre-monsoon (3.31×10^3 CFU/g) (Table 1). Actinobacterial count was found to be significant ($p < 0.01$) between sites or seasons, but not between mangrove species. Actinobacteria are distributed widely in both terrestrial and marine environments, and are widely recognized for their potential to decompose litter and produce novel bioactive metabolites such as antimicrobial, anticancer, antiviral, insecticidal, and enzyme inhibitory activities. It is worth noting that mangroves are the most fertile and productive marine ecosystem due to high microbial diversity and eco-physiological conditions^{29,49}. The present study recorded a high count of actinobacteria especially in the monsoon season ($6.57 \pm 1.61 \times 10^3$ CFU/g).

Fungal count was high in the natural mangroves at Pichavaram (6.57×10^3 CFU/g) compared to that in the planted mangroves at Vellar (6.13×10^3 CFU/g), and Ariyankuppam (6.08×10^3 CFU/g) (Table 1). The count was high in *R. apiculata* (6.29×10^3 CFU/g) followed by *A. marina* (6.23×10^3 CFU/g) (Table 1). The count varied seasonally, with the highest count in post-monsoon (7.89×10^3 CFU/g) followed by monsoon (7.21×10^3 CFU/g), summer (6.24×10^3 CFU/g), and pre-monsoon (3.71×10^3 CFU/g) (Table 1). Fungal count was found to be significant ($p < 0.01$) only between seasons, but not between mangrove sites and species. Fungi are organisms that feed on dead organic matter in mangrove environments, and play a significant role in nutrient cycling. They are among the first organisms to colonize mangrove litter, and are most abundant during the early stages of litter decomposition. Fungal colonization in mangrove litter occurs more rapidly than bacterial colonization⁴¹,

and the present study also found a high number of fungi particularly in the post-monsoon season (7.89×10^3 CFU/g). Fungi were the predominant microorganisms in the mangrove sediments, with a higher count recorded in the natural mangroves at Pichavaram (3.89×10^3 CFU/g). This increase in fungi in the mangrove sediment highlights their crucial role in the decomposition of organic matter, the production of protein-rich detritus to feed aquatic animals, and the increase of microbial carbon biomass^{4,40}.

Yeast count was found to be higher in the natural mangroves at Pichavaram (3.89×10^3 CFU/g) than in the planted mangroves at Vellar (3.56×10^3 CFU/g), and Ariyankuppam (2.84×10^3 CFU/g) (Table 1). The count was highest in *R. apiculata* (3.46×10^3 CFU/g) followed by *A. marina* (3.40×10^3 CFU/g) (Table 1). The count exhibited seasonal variation, with the highest count during the monsoon (4.48×10^3 CFU/g), followed by post-monsoon (3.77×10^3 CFU/g), summer (3.10×10^3 CFU/g), and pre-monsoon (2.37×10^3 CFU/g) (Table 1). Yeast count was found to be significant ($p < 0.01$) between sites or seasons, but not between mangrove species. Marine yeasts are ubiquitous in marine and estuarine environments, and are known for their saprophytic nature. They can play multiple roles in marine environments such as decomposition, nutrient cycling, biodegradation, and are used in a range of industrial, environmental and medical applications^{50,51}. The present study recorded high yeast counts during the monsoon ($4.48 \pm 0.79 \times 10^3$ CFU/g), due to the variety of substrates available in the mangroves especially during the monsoon, to support yeast growth^{41,52}.

Trichoderma count was higher in the natural mangroves at Pichavaram (4.74×10^3 CFU/g) than in the planted mangroves at Ariyankuppam (4.51×10^3 CFU/g), and Vellar (3.95×10^3 CFU/g) (Table 1). The count was highest in *A. marina* (4.74×10^3 CFU/g) followed by *R. apiculata* (4.44×10^3 CFU/g) (Table 1). The count showed seasonal variation with the highest count in summer (5.41×10^3 CFU/g), followed by post-monsoon (5.31×10^3 CFU/g), pre-monsoon (3.79×10^3 CFU/g), and monsoon (3.13×10^3 CFU/g) (Table 1). *Trichoderma* count was not found to be significant between sites, species, or seasons ($p < 0.01$). *Trichoderma* is a group of soil fungi, that play a vital role in soil fertility by decomposing dead plant material in mangrove forests and conserving nutrients. They can also be used as biological agent to control soil pathogens and as bio-effectors to improve plant growth in areas with high soil salinity⁵³. When associated with mangroves, *Trichoderma* species are known to help dissolve phosphate in the soil and promote the growth of *A. marina*, a species of mangrove⁵⁴. Additionally, these species have the potential to be used in bioremediation treatments⁵⁵.

Microbial counts showed seasonal variation. The counts were recorded as high during the wet-seasons. For instance, the monsoon was found to be favorable for THB, azotobacter, actinobacteria, and yeasts whereas the post-monsoon period favored lactobacillus, fungi, and thraustochytrids. This highlights the importance of wetness in regulating the microbial cycling of organic matter in mangrove soil and the flushing of land-based organic matter into mangrove habitats⁵⁶. On the other hand, the count was high in summer for cyanobacteria, and *Trichoderma*, indicating their need for high temperature and salinity for the multiplication of these microbial groups.

Thraustochytrids and other microbes in relation to physical conditions of soil

Commonly, microbial counts have increased with soil pH, salinity, temperature, and compositions of silt and clay significantly proved by the correlations among them. This showed that soil microbes were tolerant of tolerant of temperature, pH, and salinity. Hence, the microbial density changes are unaffected by sea level rise and temperature rises in mangrove soil. However, cyanobacteria were sensitive to temperature, as proved by a negative correlation between in the present study results.

Thraustochytrids are able to withstand fluctuating temperatures that prevail in the mangrove environment. They can grow within a temperature range of 0–35 °C and have a maximum temperature tolerance of up to 35 °C. However, their optimum temperature range for vegetative cell growth under culture conditions is 15–30 °C^{16,18}. The present study observed high counts of thraustochytrids in summer (27.90 ± 0.73 °C), followed by post-monsoon (25.68 ± 1.50 °C), pre-monsoon (25.43 ± 1.10 °C) and in monsoon (23.96 ± 1.20 °C), indicating their ability to tolerate a range of temperatures. Soil temperature showed a negative correlation with thraustochytrid count ($p < 0.01$) (Fig. 4a). It varied significantly between seasons, but did not vary between mangrove species or sampling sites (Table 2).

Thraustochytrids are marine obligate microbes that can grow in a wide pH range of 4–9, temperature range of 0–35 °C, and salinity of 10–70 PSU. However, they prefer neutral substrates with an optimal pH range of 6.5–7.5¹⁸, but the marine derived forms are stable with alkaline pH due to their facultative adaptation as evidenced by the negative correlation obtained between pH and thraustochytrid counts in the present study ($p < 0.01$) (Fig. 4b). Soil pH varied between seasons and sites, but not between species. It also varied with seasons, with values of 7.87 ± 0.24 in summer, 7.65 ± 0.35 in pre-monsoon, 7.65 ± 0.28 in post-monsoon, and 7.34 ± 0.13 in monsoon. Soil pH varied between sampling sites, with the highest in Ariyankuppam (7.73 ± 0.35), followed by Pichavaram (7.66 ± 0.34), and Vellar (7.50 ± 0.22) (Table 2).

In general, microbes isolated from the mangrove environment are highly salinity tolerant due to the fluctuating saline environment, as it is evidenced by the negative correlation between thraustochytrid, and pore-water salinity recorded in the present study. However, a positive correlation prevails with redox potential ($p < 0.01$) (Fig. 4c, d). This is in accordance with the report of earlier workers that thraustochytrids are euryhaline, isolated from salinities as low as 12 PSU⁵⁷. Thraustochytrids generally prefer salinities greater than 20 PSU, and less than 35 PSU for their absolute requirement of sodium ion that is not replaceable by potassium ion^{16,18}. The pore-water salinity varied between seasons and sites, but not between species. It was recorded as maximum in summer (31.64 ± 1.55 ppm) followed by post-monsoon (28.53 ± 1.66 ppm), pre-monsoon (26.16 ± 1.13 ppm), and the monsoon season (24.60 ± 1.2 ppm). The salinity was highest in Ariyankuppam (28.29 ± 2.96 ppm), followed by Pichavaram (27.54 ± 3.32 ppm), and Vellar (27.36 ± 2.78 ppm) respectively (Table 2). Soil redox potential varied between seasons and sites, but not between species. The redox potential of the soil varied with sampling sites: highest in the natural mangroves at Pichavaram (111.91 ± 15.70 mV) followed by the planted mangroves at

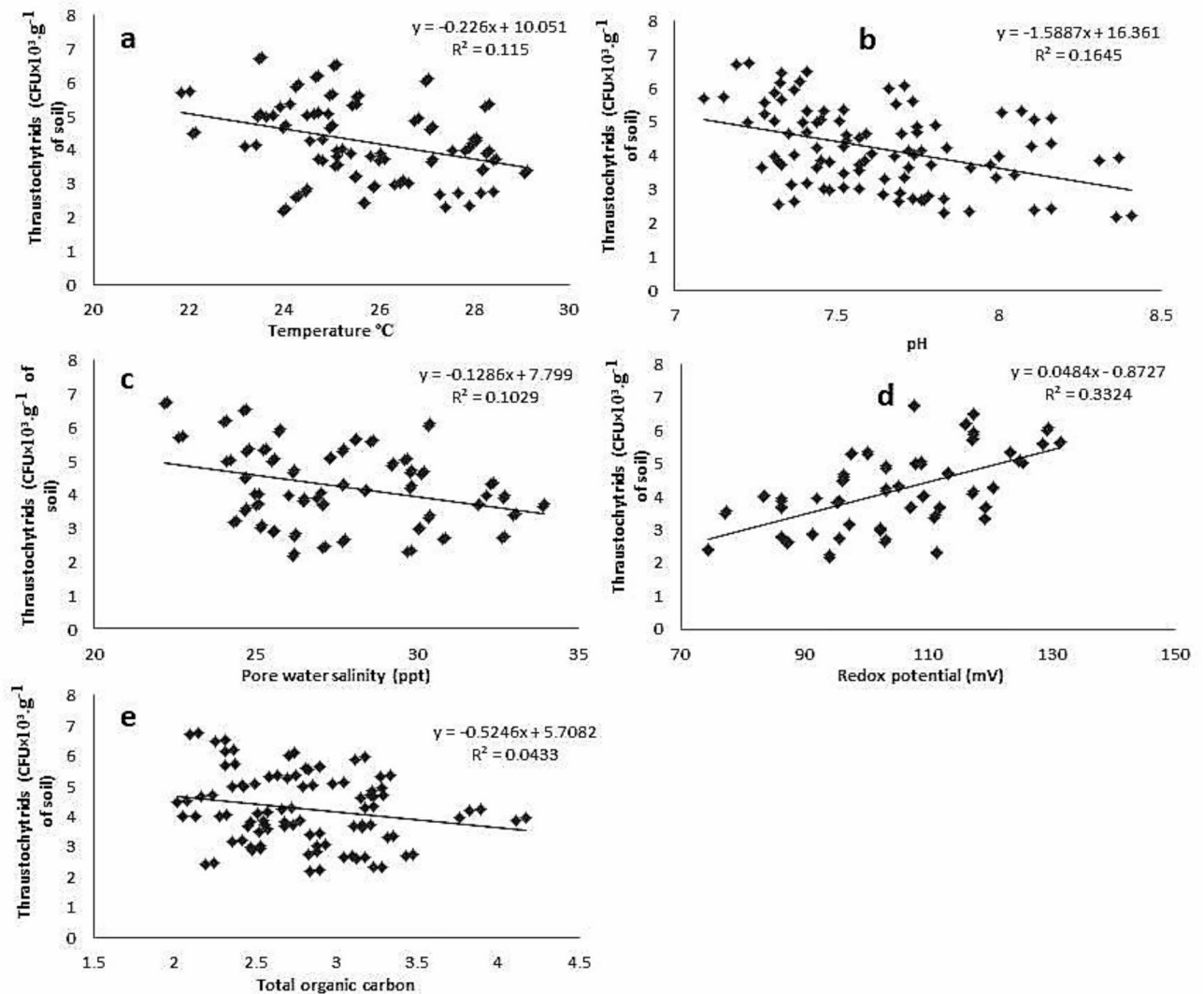


Fig. 4. Correlation between thraustochytrids count and salinity, temperature, pH and redox potential of mangrove soil.

Ariyankuppam (97.56 ± 12.16 mV) and Vellar (106.76 ± 11.95 mV). The redox potential varied between seasons: highest in the post-monsoon (117.42 ± 11.97 mV) followed by monsoon season (110.99 ± 8.97 mV), summer (102.27 ± 10.87 mV), and pre-monsoon (90.95 ± 10.83 mV) (Table 2).

Thraustochytrid count showed a positive correlation with silt, clay, and negative correlation with sand ($p < 0.01$) (Fig. 5). Sand, silt, and a clay varied only between seasons and sites, but not between mangrove species. Sand content varied between sampling sites, and it was with the highest in the planted mangroves at Vellar ($58.04 \pm 9.5\%$) followed by Ariyankuppam ($57.46 \pm 6.9\%$) and Pichavaram ($56.96 \pm 6.8\%$). The sand content was highest in the pre-monsoon ($67.86 \pm 3.6\%$) followed by summer ($60.36 \pm 1.2\%$), post-monsoon ($53.31 \pm 1.5\%$), and monsoon ($48.41 \pm 2.4\%$) (Table 2). Silt content varied between sampling locations, and it was high in the planted mangroves at Vellar ($16.88 \pm 5.3\%$) followed by Pichavaram ($16.60 \pm 5.8\%$) and Ariyankuppam ($16.46 \pm 4.4\%$). The silt content was recorded maximum in monsoon ($23.30 \pm 1.1\%$) followed by post-monsoon ($18.79 \pm 1.5\%$), summer ($14.46 \pm 1.2\%$), and pre-monsoon season ($10.03 \pm 2.0\%$) (Table 2). Clay content varied with sampling locations, with the highest in the natural mangroves at Pichavaram ($26.37 \pm 1.4\%$) followed by Ariyankuppam ($26.37 \pm 3.0\%$) and Vellar ($24.88 \pm 4.2\%$). The clay content was highest in the monsoon ($28.15 \pm 1.2\%$) followed by post-monsoon ($27.81 \pm 1.7\%$), summer ($25.08 \pm 0.9\%$), and pre-monsoon ($21.96 \pm 3.2\%$) (Table 2).

Soil texture is essential for the health of aquatic ecosystems, providing nutrients for vegetation growth and habitats for micro and macro-organisms⁵⁸. In mangroves, soil fertility comes from organic material in sediment. The abundance of fine particles with smaller diameters of silt and clay results in higher water and nutrient retention ability, as they are more active in bio-geochemical processes in soil. In contrast, sand particles with large surface areas have a deficient ability to absorb ions and water, which certainly affects the soil's ability to store water reserves and nutrients. This study shows that mangrove soil texture contains a high percentage of clay and silt, which gives it greater cohesiveness and is important from a carbon storage point of view. If the mangrove lacks water and nutrients, the plants wither, dry up and may even die^{59,60}. The grain size distribution

Source	Temperature (°C)	pH	Pore water Salinity (ppt)	Redox potential (mV)	Total Organic Carbon (mgC.g ⁻¹ soil)	Sand (%)	Silt (%)	Clay (%)	Nitrogen (g.m ⁻²)	Phosphorus (g.m ⁻²)	Potassium (g.m ⁻²)
Mangrove site											
Vellar	25.45 ± 1.8	7.50 ± 0.22	27.36 ± 2.78	106.76 ± 11.95	2.66 ± 0.37	58.04 ± 9.5	16.88 ± 5.3	24.88 ± 4.2	9.93 ± 1.69	3.72 ± 0.89	112.70 ± 4.82
Pichavaram	26.14 ± 1.6	7.66 ± 0.34	27.54 ± 3.32	111.91 ± 15.70	2.70 ± 0.38	56.96 ± 6.8	16.60 ± 5.8	26.37 ± 1.4	10.27 ± 1.9	4.11 ± 0.80	114.47 ± 5.46
Ariyankuppam	25.63 ± 1.9	7.73 ± 0.35	28.29 ± 2.96	97.56 ± 12.16	3.07 ± 0.59	57.46 ± 6.9	16.46 ± 4.4	26.00 ± 3.0	9.06 ± 1.51	2.59 ± 0.49	86.21 ± 9.28
Mangrove species											
<i>R. apiculata</i>	25.80 ± 1.84	7.66 ± 0.32	27.68 ± 3.32	105.45 ± 14.58	2.84 ± 0.37	57.53 ± 7.80	16.69 ± 5.21	25.78 ± 3.20	9.79 ± 1.80	3.50 ± 0.98	104.51 ± 4.75
<i>A. marina</i>	25.68 ± 1.83	7.60 ± 0.34	27.77 ± 2.78	105.37 ± 14.59	2.78 ± 0.38	57.45 ± 7.82	16.60 ± 5.24	25.71 ± 3.20	9.72 ± 1.80	3.44 ± 0.99	104.42 ± 4.74
Season of analysis											
Pre-monsoon	25.43 ± 1.10	7.65 ± 0.35	26.16 ± 1.13	90.95 ± 10.83	2.61 ± 0.30	67.86 ± 3.6	10.03 ± 2.0	21.96 ± 3.2	8.33 ± 0.58	2.82 ± 0.69	101.05 ± 14.65
Monsoon	23.96 ± 1.20	7.34 ± 0.13	24.60 ± 1.2	110.99 ± 8.97	2.39 ± 0.35	48.41 ± 2.4	23.30 ± 1.1	28.15 ± 1.2	10.84 ± 1.7	3.16 ± 0.86	98.76 ± 15.44
Post-monsoon	25.68 ± 1.50	7.65 ± 0.28	28.53 ± 1.66	117.42 ± 11.97	2.93 ± 0.26	53.31 ± 1.5	18.79 ± 1.5	27.81 ± 1.7	11.29 ± 1.2	3.66 ± 0.82	112.52 ± 11.27
Summer	27.90 ± 0.73	7.87 ± 0.24	31.64 ± 1.55	102.27 ± 10.87	3.30 ± 0.47	60.36 ± 1.2	14.46 ± 1.2	25.08 ± 0.9	8.57 ± 1.03	4.26 ± 0.93	105.52 ± 14.09
Site	NS	*	*	**	**	NS	NS	**	**	**	**
Species	NS	NS	NS	NS	NS	NS	NS	NS	NS	NS	NS
Season	**	**	**	**	**	**	**	**	**	**	**

Table 2. Physical and chemical characteristics of soil samples from two mangrove species of three different areas under four seasons in the year 2022–2023. Values not sharing a common superscript differ significantly at $p > 0.05$; ** = $p < 0.01$; * = $p < 0.05$; NS = Not Significant.

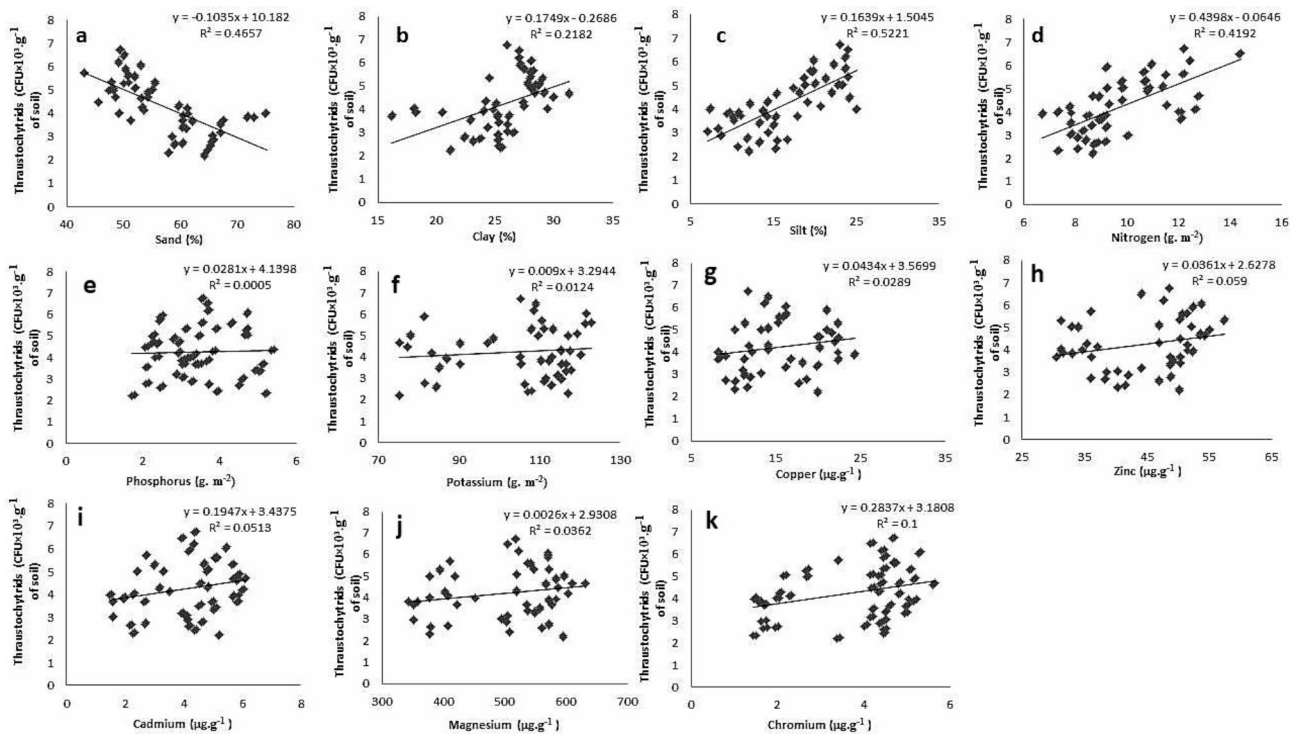


Fig. 5. Correlation between thraustochytrids count and soil texture and nutrients of mangrove soil.

differed among the three samples of sediment from mangrove-vegetation. In this study area, the mangrove sediments were primarily composed of clay particles, which accounted for $26.37 \pm 1.4\%$ in Pichavaram, whereas sand and silt particles dominated the Vellar sediment, constituting $58.04 \pm 9.5\%$ and $16.88 \pm 5.3\%$ (Table 2). The Zhangjiang Estuary mangrove wetland in China had high silt content (61–72%) and low sand content ($< 16\%$) in its sediment⁶¹. Mangrove sediment has higher concentrations of silt and clay than barren sandy soil, facilitating nutrient adsorption, microbial colonization, increasing soil fertility, and enhancing mangrove growth. The densities of all microbes increased as silt and clay levels increased, while they decreased as sand sand levels

increased⁶². The concentration of silt and clay in the sediments enhances soil fertility and promotes mangrove growth. Mangrove sediments play a vital role in nutrient biogeochemical cycles, serving as a source and sink for nutrients and organic matter owing to the activity of mangrove-associated microorganisms⁶³. The microbial population including thraustochytrids and other microbes in mangrove environments is related to the presence of organic matter in soil texture in the form of sand, silt and clay. Similarly, nutrient remineralization is based on the presence of microbial populations around the mangrove environment. This supports the present results showing higher microbial counts in the Pichavaram natural mangrove forest than the Vellar and Ariyankuppam planted mangrove sites.

Thraustochytrids and other microbes in relation to soil nutrients

Thraustochytrid count showed a negative correlation with total organic carbon (TOC) ($p < 0.01$) (Fig. 4e). Total Organic Carbon (TOC) varied between seasons, with the recorded in summer ($3.30 \pm 0.47 \text{ mgC.g}^{-1}$) followed by post-monsoon ($2.93 \pm 0.26 \text{ mgC.g}^{-1}$), pre-monsoon ($2.61 \pm 0.30 \text{ mgC.g}^{-1}$), and monsoon season ($2.39 \pm 0.35 \text{ mgC.g}^{-1}$). TOC also varied between sampling locations, with higher levels in the planted mangroves at Ariyankuppam ($3.07 \pm 0.59 \text{ mgC.g}^{-1}$) compared to Pichavaram ($2.70 \pm 0.38 \text{ mgC.g}^{-1}$) and Vellar ($2.66 \pm 0.37 \text{ mgC.g}^{-1}$). TOC of soil varied significantly between seasons and sites, but not between species (Table 2).

Soil microbial carbon constitutes the living organic matter in the soil, and also serves as the foundation for nitrogen, phosphate, and potassium. The present study found a positive correlation between total microfloral counts and microbial carbon, which is consistent with a prior finding⁶⁴. The soil carbon was recorded to be higher ($3.07 \pm 0.59 \text{ mgC.g}^{-1}$) in planted mangroves at Ariyankuppam than in the natural mangrove stand. This is due to the input of organic matter from the litter fall of mangrove trees which host an array of microorganisms⁶³. Additionally, to this, the high soil carbon around the Ariyankuppam mangrove habitat can be attributed to the inputs of sewage, and industrial discharges. Generally, planted mangroves are fast growing with an accumulation of microbes in the soil in the early stages of colonization to adjust to their new surroundings⁵⁴. Soil microorganisms are crucial for storing carbon in mangrove habitats, and hence soil organic carbon is an indicator of productivity⁶⁴. Therefore, it is important to maintain a high density of these microbes by preserving dense mangrove forests.

In the present study, thraustochytrid counts positively correlated with soil nutrients such as nitrogen, potassium, and phosphorus (Fig. 5). Levels of N, P, K in the soil varied significantly between sites and seasons, but not between mangrove species (Table 2). Soil nitrogen was high in the natural mangroves at Pichavaram ($10.27 \pm 1.9 \text{ g.m}^{-2}$) followed by the planted sites at Vellar ($9.93 \pm 1.69 \text{ g.m}^{-2}$), and Ariyankuppam ($9.06 \pm 1.51 \text{ g.m}^{-2}$). The soil nitrogen was also high in the post-monsoon season ($11.29 \pm 1.2 \text{ g.m}^{-2}$) followed by monsoon ($10.84 \pm 1.7 \text{ g.m}^{-2}$), summer ($8.57 \pm 1.03 \text{ g.m}^{-2}$), and pre-monsoon season ($8.33 \pm 0.58 \text{ g.m}^{-2}$). Soil phosphorus was high in the natural mangroves at Pichavaram ($4.11 \pm 0.80 \text{ g.m}^{-2}$) followed by planted mangroves at Vellar ($3.72 \pm 0.89 \text{ g.m}^{-2}$), and Ariyankuppam ($2.59 \pm 0.49 \text{ g.m}^{-2}$). The soil phosphorus was also high in summer ($4.26 \pm 0.93 \text{ g.m}^{-2}$) followed by post-monsoon ($3.66 \pm 0.82 \text{ g.m}^{-2}$), monsoon ($3.16 \pm 0.86 \text{ g.m}^{-2}$), and pre-monsoon season ($2.82 \pm 0.69 \text{ g.m}^{-2}$). Soil potassium was maximum in the post-monsoon season ($112.52 \pm 11.27 \text{ g.m}^{-2}$), followed by summer ($105.52 \pm 14.09 \text{ g.m}^{-2}$), pre-monsoon ($101.05 \pm 14.65 \text{ g.m}^{-2}$), and minimum in the monsoon season ($98.76 \pm 15.44 \text{ g.m}^{-2}$). Soil potassium was higher in the natural mangroves at Pichavaram ($114.47 \pm 5.46 \text{ g.m}^{-2}$) than in the planted mangroves at Vellar ($112.70 \pm 4.82 \text{ g.m}^{-2}$), and Ariyankuppam ($86.21 \pm 9.28 \text{ g.m}^{-2}$).

The high levels of N, P, K in the soil may be due to the presence of nitrogen fixing microbes such as cyanobacteria, azotobacters, and phosphate solubilising fungi, and *Trichoderma* in the natural mangroves, as compared to the planted mangroves. This is similar to an earlier finding that soil nutrients are several folds higher in planted mangroves due to the abundance of nutrient fixing microbes than in barren habitat⁴¹. Mangrove biotopes are generally nutrient-limited due to high salinity that interferes with the availability of soluble nutrients to plants⁵⁶. Mangrove associated soil microbes are important contributors to nutrient cycles for N, P, Sulphur, and Carbon in mangrove habitats. In the present study, the planted mangroves exhibited higher levels of K ($114.47 \pm 5.46 \text{ g.m}^{-2}$) and P ($4.11 \pm 0.80 \text{ g.m}^{-2}$) than the natural mangroves. Microbial communities contribute significantly to nutrient enrichment in mangrove biotopes by increasing soil carbon and nitrogen levels by up to 49%⁶⁵. Moreover, the microbes convert insoluble nutrients into soluble ones to enhance the bioavailability of nutrients for the better growth of mangrove plants⁵⁴. The bioavailability of nutrients in the soil is controlled by factors such as pH, redox potential, and salinity⁶². The present work recorded temporal variation in, thraustochytrids being high in the post-monsoon season, followed by monsoon, summer and pre-monsoon. This microbial abundance in the post-monsoon can be attributed to the availability of organic substrates for decomposition by the saprophytic microbes and higher availability of nutrients (N, P, K) in support of mangroves and associated organisms.

Levels of Cu, Zn, Mn, Cr and Cd in the soil varied significantly between sites and seasons, but not between mangrove species (Table 3). Soil Cu was found higher ($20.90 \pm 1.86 \text{ } \mu\text{g.g}^{-1}$) in Vellar than that ($10.98 \pm 2.34 \text{ } \mu\text{g.g}^{-1}$) in Ariyankuppam site. Soil Cu ranged between 13.06 ± 4.38 , and $16.42 \pm 5.40 \text{ } \mu\text{g.g}^{-1}$ at different seasons: supreme in summer and least in pre-monsoon (Table 3). Soil Zn was higher ($51.83 \pm 2.65 \text{ } \mu\text{g.g}^{-1}$) in Vellar than ($34.79 \pm 2.99 \text{ } \mu\text{g.g}^{-1}$) in Ariyankuppam. Soil Zn ranged between 40.78 ± 7.40 and $47.04 \pm 8.96 \text{ } \mu\text{g.g}^{-1}$ at different seasons: highest in post-monsoon and lowest in pre-monsoon (Table 3). Soil Mn was found to be higher ($583.76 \pm 21.64 \text{ } \mu\text{g.g}^{-1}$) in Vellar than that ($389.44 \pm 31.50 \text{ } \mu\text{g.g}^{-1}$) in Ariyankuppam. Soil Mn ranged between 477.25 ± 2.69 to $512.81 \pm 8.60 \text{ } \mu\text{g.g}^{-1}$ at different seasons: highest in monsoon and lowest in pre-monsoon (Table 3). Soil Cr was higher ($4.64 \pm 0.56 \text{ } \mu\text{g.g}^{-1}$) in Vellar than in Ariyankuppam ($2.02 \pm 0.55 \text{ } \mu\text{g.g}^{-1}$). Soil Cr varied between 3.34 ± 1.30 and $3.98 \pm 1.45 \text{ } \mu\text{g.g}^{-1}$ during different seasons. The Cr concentration was observed uppermost during post-monsoon, least during pre-monsoon (Table 3). Soil Cd was higher ($5.30 \pm 0.71 \text{ } \mu\text{g.g}^{-1}$) in Vellar than in Ariyankuppam ($2.43 \pm 0.66 \text{ } \mu\text{g.g}^{-1}$). It ranged between 3.58 ± 1.21 and $4.72 \pm 1.20 \text{ } \mu\text{g.g}^{-1}$ at different seasons: highest in post-monsoon and lowest in pre-monsoon (Table 3).

Source	Micro nutrients ($\mu\text{g.g}^{-1}$)				
	Cu	Zn	Mn	Cr	Cd
Mangrove site:					
Vellar	10.98 \pm 2.34	34.79 \pm 2.99	389.44 \pm 31.50	2.02 \pm 0.55	2.43 \pm 0.66
Pichavaram	14.48 \pm 2.42	47.24 \pm 3.98	526.06 \pm 21.88	4.54 \pm 0.33	4.64 \pm 0.48
Ariyankuppam	20.90 \pm 1.86	51.83 \pm 2.65	583.76 \pm 21.64	4.64 \pm 0.56	5.30 \pm 0.71
Mangrove species:					
<i>R.apiculata</i>	15.48 \pm 4.71	44.66 \pm 7.98	499.78 \pm 86.40	3.76 \pm 1.32	4.15 \pm 1.39
<i>A.marina</i>	15.42 \pm 4.71	44.59 \pm 7.98	499.72 \pm 86.40	3.70 \pm 1.32	4.09 \pm 1.39
Season of analysis:					
Pre-monsoon	13.06 \pm 4.38	40.78 \pm 7.40	477.25 \pm 2.69	3.34 \pm 1.30	3.58 \pm 1.24
Monsoon	16.01 \pm 4.00	44.55 \pm 8.21	512.81 \pm 8.60	3.84 \pm 0.90	3.85 \pm 1.21
Post-monsoon	16.31 \pm 4.34	47.04 \pm 8.96	509.31 \pm 2.14	3.98 \pm 1.45	4.72 \pm 1.20
Summer	16.42 \pm 5.40	46.12 \pm 5.99	499.64 \pm 1.70	3.78 \pm 1.52	4.34 \pm 1.63
Site	**	**	**	**	**
Species	NS	NS	NS	NS	NS
Season	**	**	**	**	**

Table 3. Levels of micronutrients in mangrove soil of two mangrove species from three different sites under four seasons in the year 2022–2023. Values not sharing a common superscript are differ significantly at $p > 0.05$; ** = $p < 0.01$; * = $p < 0.05$; NS = Not Significant.

Microbial communities are highly dependent on soil conditions. In the present study, thraustochytrid counts positively correlated with micronutrients of Cr, Cu, Mg, Cd, and Zn (Table 2; Fig. 5). The micronutrients accumulated at higher levels in natural mangroves than in planted mangroves. The micronutrients get accumulated in the mangrove soil during the litter decomposition process⁴¹. In addition to this natural process, industrial discharges are likely to contaminate the mangrove habitat, as is true with the planted site at Ariyankuppam that exhibited higher levels of micronutrients (Cu, Zn, Mn, Cr, and Cd) than other sites (Table 3).

In general, micronutrients showed a positive effect on the growth enhancement, cell proliferation, and morphological changes of thraustochytrids and these effects varied with the microbial strains and concentration of micronutrients. The concentration of Cu (II) from 2 to 16 ppm is reported to support the sporulation and growth of thraustochytrids but to have a strong negative effect at higher concentrations. For instance, at 512 ppm, thraustochytrids do not produce zoospores⁶⁶. Thraustochytrids are shown to have positive cell growth and cell proliferation in the existence of heavy metals such as Mn, Zn, Ni, Cu, Cd, and Cr at concentrations below 500 ppm, but at higher concentrations the metals reduce colony size along with depression or holes in the cell wall¹⁵. Thus, the micronutrients are a potential nutrient source for the growth of thraustochytrids, revealing their potential for heavy metal bioremediation. In addition, the trace elements did not affect the thraustochytrid count, indicating their potential for metal tolerance (Fig. 6).

Morphological and molecular identification of thraustochytrids

Thraustochytrids were observed to grow as white, pale white, light pink, or cream-colored colonies in GYP media. In this study, 113 thraustochytrid strains were isolated from mangrove habitats. Of these, only 48 pure cultures survived after three rounds of sub-culturing. Based on survival, color, and shape, two isolates from each sampling site in each season were selected. The 24 predominant isolates were then identified based on their morphological features such as colour, shape, single cells, triploid, tetrapod, or cluster of cells and various forms of cell structure, observed under a light and scanning electron microscope as shown in Figs. 7, 8 and 9. Additional observations were also recorded for the presence of motile zoospores, amoeboid cells, formation of an ectoplasmic network, and binary cell division (Table 4; Figs. 7, 8 and 9). Reproduction was observed once cells had fully developed and undergone successive sequential binary division. Based on these morphological features, the isolates were identified under five genera viz., *Thraustochytrium*, *Aurantiochytrium*, *Botryochytrium*, *Parietichytrium*, and *Schizochytrium* (Fig. 6)¹. Identification at the species level is challenging due to overlapping morphological characteristics. Hence, we employed the 18 S rDNA sequencing as it is crucial for accurate identification. However, a significant limitation is in the molecular identification is the lack of comprehensive reference for a comprehensive gene sequence in the GenBank.

In the present study, 24 thraustochytrid isolates were molecularly identified using 18 S rRNA sequencing (Table 4). The partial 18 S rRNA sequences, analyzed using NCBI BLAST, confirmed the systematic positions of the isolates with similarity ranging from 93.36 to 99.09% to known thraustochytrid sequences. These sequences were submitted to the NCBI GenBank with accession numbers PQ213052, PQ213058, PQ213062, PQ213067, PQ213090, PQ213092, PQ213097, PQ213099, PQ213100, PQ213360, PQ213261, PQ213441, PQ213443, PQ213444, PQ213448, PQ213449, PQ213450, PQ213451, PQ213453, PQ213454, PQ213455, PQ213456, PQ213460, and PQ213461 (Table 1). The results indicated that the mangrove soil associated thraustochytrid strain, *Thraustochytrium* sp. PVTSK-01 (Accession No. PQ213092), exhibited 96.51% similarity to *Thraustochytrium* sp. PJA10 (DQ834734), and 93.56% similarity with *Thraustochytriidae* sp. MBIC11074 (AB290579). *Thraustochytrium* sp. PVTSK-02 (Accession No. PQ213099), exhibited 98.52% similarity to

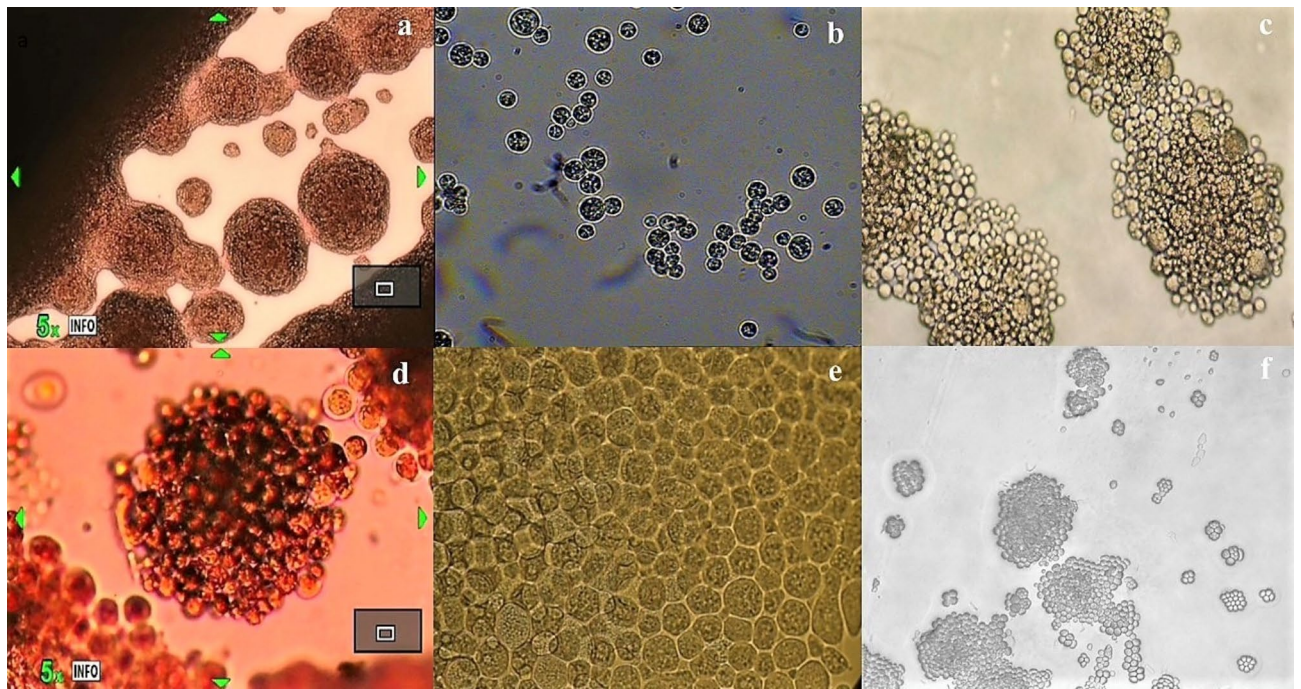


Fig. 6. Pure colonies of thraustochytrids taken with light microscopy (a) Colony morphology of thraustochytrid under 4 × magnification, (b) *Schizochytrium* (PVTSK-06), (c) *Aurantiochytrium* (AKTSK-06), (d) *Thraustochytrium* (VRTSK-08), (e) *Parietichytrium* (VRTSK-06), and (f) *Botryochytrium* (PVTSK-07) under 40 × magnifications.

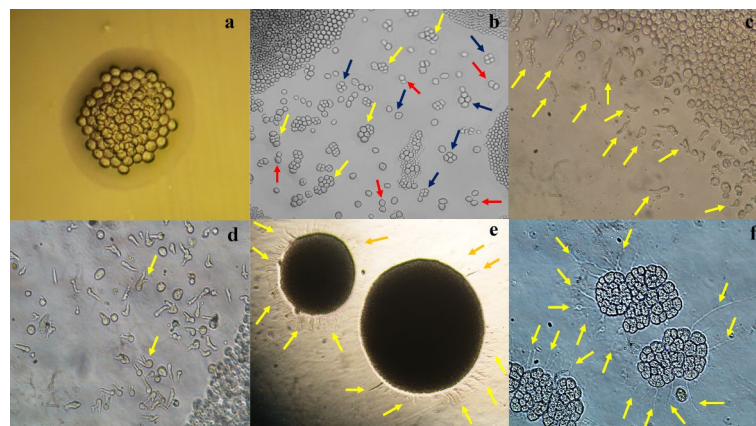


Fig. 7. Developmental stages of thraustochytrids observed under light microscopy, (a) Clusters of vegetative cells (40 ×), (b) Clusters of vegetative cells dividing through binary fission, with 4, 6, and 8 cells (40 ×), (c) Clusters of vegetative cells containing numerous intracellular zoospores (40 ×), (d) Many spherical or limaciform amoeboid cells (40 ×), (e) Filamentous ectoplasmic net elements around the vegetative cells (4 ×), (f) filaments of the ectoplasmic network surrounding larger vegetative cells undergoing binary division with the visible ectoplasmic network (100 ×).

Thraustochytrium aureum strain BT6 (OP177664), and 98.24% similarity with *Thraustochytrium aureum* N5998 (OQ514335). *Aurantiochytrium* sp. VRTSK-01 (Accession No. PQ213455), exhibited 97.03% similarity to *Aurantiochytrium* sp. TK7 (OK244291), and 86.19% similarity with *Aurantiochytrium* sp. TK7 (OK244288). *Thraustochytrium* sp. VRTSK-02 (Accession No. PQ213097), exhibited 97.83% similarity to *Thraustochytrium* sp. LY-2012 (JX847374), and 97.08% similarity with *Thraustochytrium* sp. BL8 (FJ821488). *Aurantiochytrium* sp. AKTSK-01 (Accession No. PQ213360), exhibited 94.59% similarity to *Aurantiochytrium* sp. TK2 (OK244286), and 87.11% similarity with *Aurantiochytrium* sp. TK9 (K244293).

Aurantiochytrium sp. AKTSK-02 (Accession No. PQ213441), exhibited 95% similarity to *Aurantiochytrium* sp. UMACC-T005 (KP015179), and 94.79% similarity with *Aurantiochytrium limacinum* (AB810940).

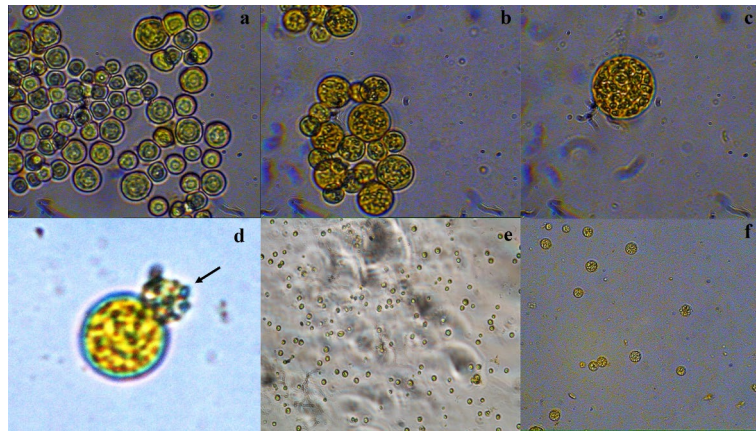


Fig. 8. Developmental stages of thraustochytrids observed under light microscopy, (a) Clusters of vegetative cells (40 ×), (b) Mature zoosporangium (40 ×), (c) Mature with active zoospores about to release (40 ×), (d) Release of zoospores from zoosporangium, (e) Many active zoospores (40 ×), (f) Young vegetative cells formed by encystment of zoospores (40 ×).

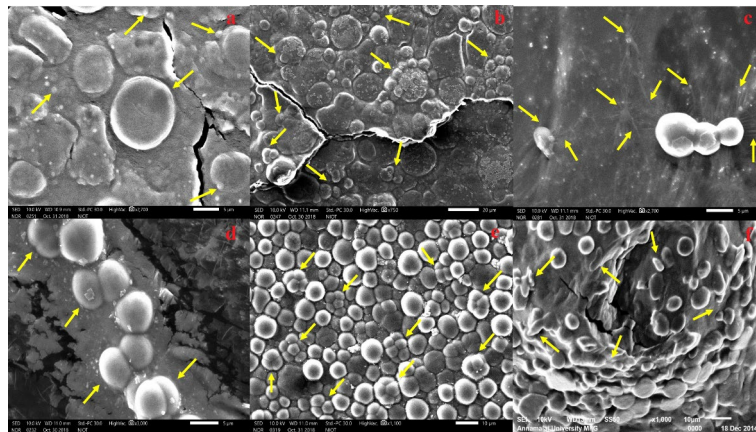


Fig. 9. Developmental stages of thraustochytrids seen under scanning electron microscopic observation, (a) Mature vegetative cells, (b) Mature zoosporangium releasing zoospores, (c) Filaments of the ectoplasmic network, (d) Clusters of vegetative cells dividing through binary fission, forming diad cells, (e) Clusters of vegetative cells dividing through binary fission, forming groups of 4, 6, and 8 cells, (f) Clusters of vegetative cells with reniform or ovoid shape of zoospore and amoeboid cells.

Aurantiochytrium sp. VRTSK-03 (Accession No. PQ213456), exhibited 97.96% similarity to *Aurantiochytrium* sp. TK2 (OK244286), and 88.61% similarity with *Aurantiochytrium* sp. TK9 (K244293). *Aurantiochytrium* sp. VRTSK-04 (Accession No. PQ213461), exhibited 97.03% similarity to *Aurantiochytrium mangrovei* strain BT3 (OP175985), and 96.96% similarity with *Schizochytrium mangrovei* (DQ367049). *Aurantiochytrium* sp. AKTSK-03 (Accession No. PQ213444), exhibited 96.36% similarity to *Aurantiochytrium* sp. T7(LC651621), and 96.24% similarity with *Aurantiochytrium limacinum* (AB810938). *Thraustochytrium* sp. AKTSK-04 (Accession No. PQ213090), exhibited 99.09% similarity to *Thraustochytrium* sp. MBT12 (MK615598), and 98% similarity with *Thraustochytrium* sp. AR2-19 (AB810951). *Aurantiochytrium* sp. PVTSK-03 (Accession No. PQ213454), exhibited 93.36% similarity to *Aurantiochytrium* sp. MBT03A (MH595610), and 92.84% similarity with *Aurantiochytrium acetophilum* (MH319333). *Schizochytrium* sp. PVTSK-04 (Accession No. PQ213062), exhibited 98.94% similarity to *Schizochytrium* sp. isolate TK10 (OK244294), and 88.01% similarity with *Schizochytrium* sp. ABC101 (MK265698). *Thraustochytrium* sp. VRTSK-05 (Accession No. PQ213100), exhibited 97.61% similarity to *Thraustochytrium kinnei* (KF460465), and 96.22% similarity with *Thraustochytriidae* sp. MBIC11093 (AB183664). *Parietichytrium* sp. VRTSK-06 (Accession No. PQ213058), exhibited 98.32% similarity to *Parietichytrium* sp. TF79 (KM023708), and 97.21% similarity with *Thraustochytriidae* sp. MBIC11085 (AB290580).

Aurantiochytrium sp. AKTSK-05 (Accession No. PQ213443), exhibited 98.29% similarity to *Aurantiochytrium* sp. CMFRIMBTJMV7 (MH059484), and 97.91% similarity with *Aurantiochytrium limacinum* (AB810939). *Aurantiochytrium* sp. AKTSK-06 (Accession No. PQ213448), exhibited 97.63% similarity to *Aurantiochytrium* sp. MBT03A (MH595610), and 97.15% similarity with *Aurantiochytrium limacinum* (AB810939). *Aurantiochytrium*

Isolate No	Colony morphology	Cell wall	Binary cell division	Amoeboid cell	Ectoplasmic network	Organism's name	NCBI accession number
VRTSK-01	Creamy white, larger spherical shape colonies, cluster of vegetative cells, biflagellate zoospores	Thin	Present	Present	Well developed	<i>Aurantiochytrium</i> sp.	PQ213455
VRTSK-02	Creamy white, medium oblong shape colonies, Internal proliferation with motile zoospore formation	Thick	Absent	Absent	Absent	<i>Thraustochytrium</i> sp.	PQ213097
AKTSK-01	Creamy orange, moderate round shape thallus, 2,4,8 and different numbers of vegetative cells	Thin	Present	Present	Well developed	<i>Aurantiochytrium</i> sp.	PQ213360
AKTSK-02	White, medium globes, and spherical shape colonies, bi-partition cleavage, diads, tetrads, and different numbers of vegetative cells, ovoid zoospores	Thin	Present	Present	Well developed	<i>Aurantiochytrium</i> sp.	PQ213441
PVTSK-01	Orange, small to large globes and sub- globes colonies, motile zoospore formation	Thin	Absent	Present	Un developed	<i>Thraustochytrium</i> sp.	PQ213092
PVTSK-02	White, small spherical or sub-spherical thallus, zoosporangia contain large vesicle, many active zoospore	Thick	Present	Present	Well developed	<i>Thraustochytrium</i> sp.	PQ213099
VRTSK-03	Pale white, globes, and sub-globes thallus, 2,4,7 and different numbers of vegetative cells present, amoeboid cells present	Thick	Absent	Present	Absent	<i>Aurantiochytrium</i> sp.	PQ213456
VRTSK-04	Creamy orange, small to very large round colonies, 2,4, and different numbers of vegetative cells present, oval shape active zoospore	Thin	Present	Present	Poorly developed	<i>Aurantiochytrium</i> sp.	PQ213461
AKTSK-03	Pale white, medium globes or sub-globse or round colonies, bi-partition cleavage, tetrads, spherical shape zoospores	Thin	Present	some cell present	Well developed	<i>Aurantiochytrium</i> sp.	PQ213444
AKTSK-04	Creamy white, moderate round shape colonies, zoosporangia contain large vesicles, and multiproliferous bodies many active zoospore	Thin	Present	Present	Absent	<i>Thraustochytrium</i> sp.	PQ213090
PVTSK-03	White, small to medium globes or sub- globes shape of cell, diads, tetrads, and different numbers of cells division stage present	Thin	Present	Present	Well developed	<i>Aurantiochytrium</i> sp.	PQ213454
PVTSK-04	Pale white, medium spherical or pseudopodia shape of cell, bi-partition cleavage, 2,4, and different numbers of vegetative cells present, reniform or ovoid shape zoospores	Thin	Present	Present	Well developed	<i>Schizochytrium</i> sp.	PQ213062
VRTSK-05	Pale white, medium oblong or sub-oblong shape cells, Internal proliferation with motile zoospore formation, presence of biflagellate zoospores	Thin and Thick	Present	Present	Well developed	<i>Thraustochytrium</i> sp.	PQ213100
VRTSK-06	Creamy white, large globes and sub globes thallus. binary cell division and active zoospores present	Thick	Absent	Absent	Absent	<i>Parietichytrium</i> sp.	PQ213058
AKTSK-05	Orange, larger thin wall globes or spherical shape of thallus, binary cell partition, 2, 4, 8 cluster of vegetative cells, biflagellate zoospores	Thin	Present	Present	Well developed	<i>Aurantiochytrium</i> sp.	PQ213443
AKTSK-06	White, medium round or globes or sub-globse, bi-partition cleavage, tetrads, spherical shape zoospores	Thin	Present	Present	Well developed	<i>Aurantiochytrium</i> sp.	PQ213448
PVTSK-05	Creamy white, medium to large pseudopodia or spherical shape of cell, zoosporangia contain large vesicle, many active zoospore	Thick	Absent	Present	Un-developed	<i>Aurantiochytrium</i> sp.	PQ213451
PVTSK-06	Orange, small to large globes and sub-globes thallus, 2,4 and different numbers of vegetative cells present, reniform or ovoid shape active zoospores present	Thin	Present	Present	Well developed	<i>Schizochytrium</i> sp.	PQ213067
VRTSK-07	Creamy orange, small to large round shape thallus, Pseudopodia or Spherical shape of cell, oval shape zoospores actively present	Thick	Absent	Present	Absent	<i>Aurantiochytrium</i> sp.	PQ213460
VRTSK-08	White, small round or spherical thallus, Multiproliferous bodies, zoosporangia contain large vesicles	Thin	Present	Absent	Poorly developed	<i>Thraustochytrium</i> sp.	PQ213261
AKTSK-07	Pale white, medium to large round shape colonies, bi-partition several times before heterokont zoospores formed	Thin	Present	some cell present	Well developed	<i>Aurantiochytrium</i> sp.	PQ213449
AKTSK-08	Orange, small to medium globes or sub- globes shape of cell, bi-partition cleavage present, diads, tetrads, and different numbers of cells present	Thick	Absent	Present	Un-developed	<i>Aurantiochytrium</i> sp.	PQ213450
PVTSK-07	Creamy orange, larger spherical or sub-spherical shape thallus, Internal proliferation with motile and biflagellate zoospore formation	Thin and Thick	Absent	Present	Un branched and not well developed	<i>Botryochytrium</i> sp.	PQ213052
PVTSK-08	Pale white, medium spherical or pseudopodia shape of cell, 2,4, and different numbers of vegetative cells present, different shape of zoospores cells presents	Thin	Present	Present	Well developed	<i>Aurantiochytrium limacinum</i>	PQ213453

Table 4. Morphological characters of the newly isolated thraustochytrids from mangrove soil and accession number used in 18 S rRNA gene sequences.

sp. PVTSK-05 (Accession No. PQ213451), exhibited 95.35% similarity to *Aurantiochytrium* sp. ICTFD5 (MK547272), and 95.16% similarity with *Aurantiochytrium* sp. KRS101 (HM126528). *Schizochytrium* sp. PVTSK-06 (Accession No. PQ213067), exhibited 97.30% similarity to *Schizochytrium* sp. KK-2016 (KT716338), and 96.76% similarity with *Schizochytrium* sp. LU310 (KM245569). *Aurantiochytrium* sp. VRTSK-07 (Accession No. PQ213460), exhibited 94.60% similarity to *Aurantiochytrium* sp. TK7 (OK244291), and 84.61% similarity with *Aurantiochytrium* sp. TK4 (OK244288). *Thraustochytrium* sp. VRTSK-08 (Accession No. PQ213261), exhibited 94.60% similarity to *Aurantiochytrium* sp. TK7 (OK244291), and 84.61% similarity with *Aurantiochytrium* sp. TK4 (OK244288). *Aurantiochytrium* sp. AKTSK-07 (Accession No. PQ213449), exhibited 97.64% similarity to *Aurantiochytrium* sp. CMFRIMBTJMV7 (MH059484), and 97.51% similarity with *Thraustochytriidae* sp.

NIOS-1 (AY705776). *Aurantiochytrium* sp. AKTSK-08 (Accession No. PQ213450), exhibited 94.03% similarity to *Aurantiochytrium* sp. DDH7 (ON128279), and 94.02% similarity with *Aurantiochytrium limacinum* (AB810940). *Botryochytrium* sp. (PVTSK-07 (Accession No. PQ213052), exhibited 98.95% similarity to *Botryochytrium* sp. MBT01 (MH349018), and 98.64% similarity with *Botryochytrium* sp. TMR16-11 (AB810986). *Aurantiochytrium limacinum* PVTSK-08 (Accession No. PQ213453), exhibited 95.14% similarity to *Aurantiochytrium* sp. TF93 (KM023704), and 94.58% similarity with *Aurantiochytrium limacinum* (KM023701) (Table 4).

The BLAST results revealed high 18 S rRNA sequence similarity with other thraustochytrid strains in the GenBank database. The high sequence similarity suggests a ubiquitous nature of thraustochytrids. Phylogenetic analysis supported the taxonomic positions of these species with identities ranging from 93.43 to 100%. Strains with full-length 18 S sequence identities below 92% may represent distinct genera, those between 92% and 97% are likely congeneric species, and identities exceeding 97% support species-level identification^{34,67}. Further research, including whole-genome sequencing, is necessary for clearer taxonomic resolution at the species level. Among the genera, *Aurantiochytrium* was the predominant genus across all sampling sites and seasons, followed by *Thraustochytrium*. The high sequence similarity indicates the widespread presence of thraustochytrids. *Botryochytrium* (PVTSK-07) was found to be present in Pichavaram during summer, *Parietichytrium* (VRTSK-06) was found to be present in Vellar during post-monsoon, while *Schizochytrium* (PVTSK-04, PVTSK-06) in Pichavaram during the monsoon and post-monsoon.

Thraustochytrids are abundant for different seasons from coastal waters of southern China⁶⁸. *Aurantiochytrium* species are reported to be predominant in decomposing leaves in Malaysian mangroves⁹. The same species is observed more frequently (57.50%) in mangrove habitats during the summer and monsoon seasons in Thailand¹¹ (Jaritkhuan and Suanjit 2018). Similarly, *Aurantiochytrium* is reported to be the most dominant and fast-growing genus of thraustochytrids in Kerala, Mumbai and Andaman mangrove regions of India^{5,16,18}. The present work recorded that *Aurantiochytrium* was abundant by 61% of thraustochytrids, which is similar to a recent report on six closely related genera of labyrinthulomycete, discovered from coastal mangrove habitats of China⁷. The morphological and molecular features of all isolates are detailed in Table 4. Most isolates accumulated relatively low levels of arachidonic acid, but strains PVTSK-02 and AKTSK-04 had concentrations of less than 1%, which is characteristic of *Thraustochytrium* species. The genus-level phylogenetic groups within the Labyrinthulomycetes are distinguished by a combination of morphological and molecular features, although identifying each group based on a single feature remains challenging. The cultured diversity represents only a fraction of their actual diversity, highlighting the need for novel culture methods and studies of uncultured thraustochytrid diversity.

Biomass production and total lipid content in thraustochytrids

Data on biomass and lipid content of thraustochytrids are shown in Fig. 10a, b and the values varied between isolates or seasons. Biomass production ranged from 4.35 to 15.71 g/L with a high range of values (8.46 to 15.71 g/L) in the post-monsoon season compared to other seasons: summer (8.53 to 13.68 g/L) and monsoon (7.76 to 14.74 g/L). Among the isolates, *Aurantiochytrium* sp. (AKTSK-06) produced the highest biomass of 15.71 g/L while *Thraustochytrium* sp. (VRTSK-02) had the lowest biomass of 4.35 g/L.

Total lipid ranged from 26.78 to 61.33% of dry cell weight, as shown in Fig. 10b. The total lipid content was in a high range of 39.87–61.33% in the strains isolated in the monsoon, followed by post-monsoon (31.78–57.24%), summer (34.33–48.14%), and pre-monsoon isolates (26.78–45.46%). Among the isolates, *Aurantiochytrium* sp. (PVTSK-03) accumulated the highest lipid content of 61.33%, while *Thraustochytrium* sp. (VRTSK-02) had the lowest lipid content of 26.78%. The lipid content was higher in *Aurantiochytrium* than in *Schizochytrium* and *Thraustochytrium*, which is similar to previous reports^{18,69}. In general, thraustochytrids exhibited high biomass and lipid content in all four seasons of the year due to their fast-growing nature.

The present work recorded high levels of biomass and lipid in thraustochytrids, compared to earlier reports of the Indian subcontinent. Gupta et al., recorded biomass of 1.10–3.64 g/L with a lipid content of approximately 30% in 19 strains of thraustochytrid strains from Goa⁶⁹. Similarly, Jaseera et al., reported biomass of 7.3–10.6 g/L with a lipid content of 12% in 11 strains isolated from Kerala¹⁶. However, some earlier studies reported higher values, comparable to the present work. The biomass production ranged from 6.88 to 22.49 g/L for *Aurantiochytrium mangrovei* and 9.39 to 20.71 g/L for *A. limacinum* isolated from Thailand¹¹. Similarly, biomass production was reported in a range of 14.12 ± 0.69–22.98 ± 0.53 g/L with lipid content in a range of 42.65–58.86% for strains isolated from Mumbai⁵. The biomass production in 33 Malaysian strains of thraustochytrids reportedly varied from 1.07 to 5.82 g/L, and the lipid content from 3.29–15.76%⁹. A recent study recorded the highest biomass of 5.42 g/L in ANVKK-06 and lipid content of 71.03% in ANVKK-03 among 127 strains isolated from Andaman mangroves¹⁸.

Thraustochytrids require suitable nutrients (carbon and nitrogen) to achieve high levels of biomass and lipid, under optimal conditions of pH, temperature, salinity and incubation time. The present study used glucose, peptone, and yeast extract as sources of carbon and nitrogen to enhance biomass and lipid production, based on earlier works^{18,70}. The strain *A. limacinum* SR21 is reported to produce a biomass of 3.4 ± 0.4 g/L in a fed-batch culture. However, when grown under optimized culture conditions for 7 days, the same strain yields 4.2-fold higher biomass of 14.3 ± 0.5 g/L⁷¹. Therefore, biomass yield may vary with thraustochytrid strains, optimal growth conditions, and nutrient sources.

Fatty acid composition in thraustochytrids

The fatty acid profiles of thraustochytrids exhibited significant variations with different seasons, as shown in Fig. 11a, b, c, and d. Two main types of fatty acids, namely, saturated fatty acids (SFAs) and long-chain polyunsaturated fatty acids (LC-PUFAs) were present. The most abundant SFAs was palmitic acid (C16:0) (26.15–44.21%), followed by pentadecanoic acid (C15:0), myristic acid (C14:0), arachidic acid (C20:0), and stearic acid (C18:0), with relative abundance of 3.29–10.89%, 1.02–9.08%, 0.14–6.34% and 0.08–3.23%,

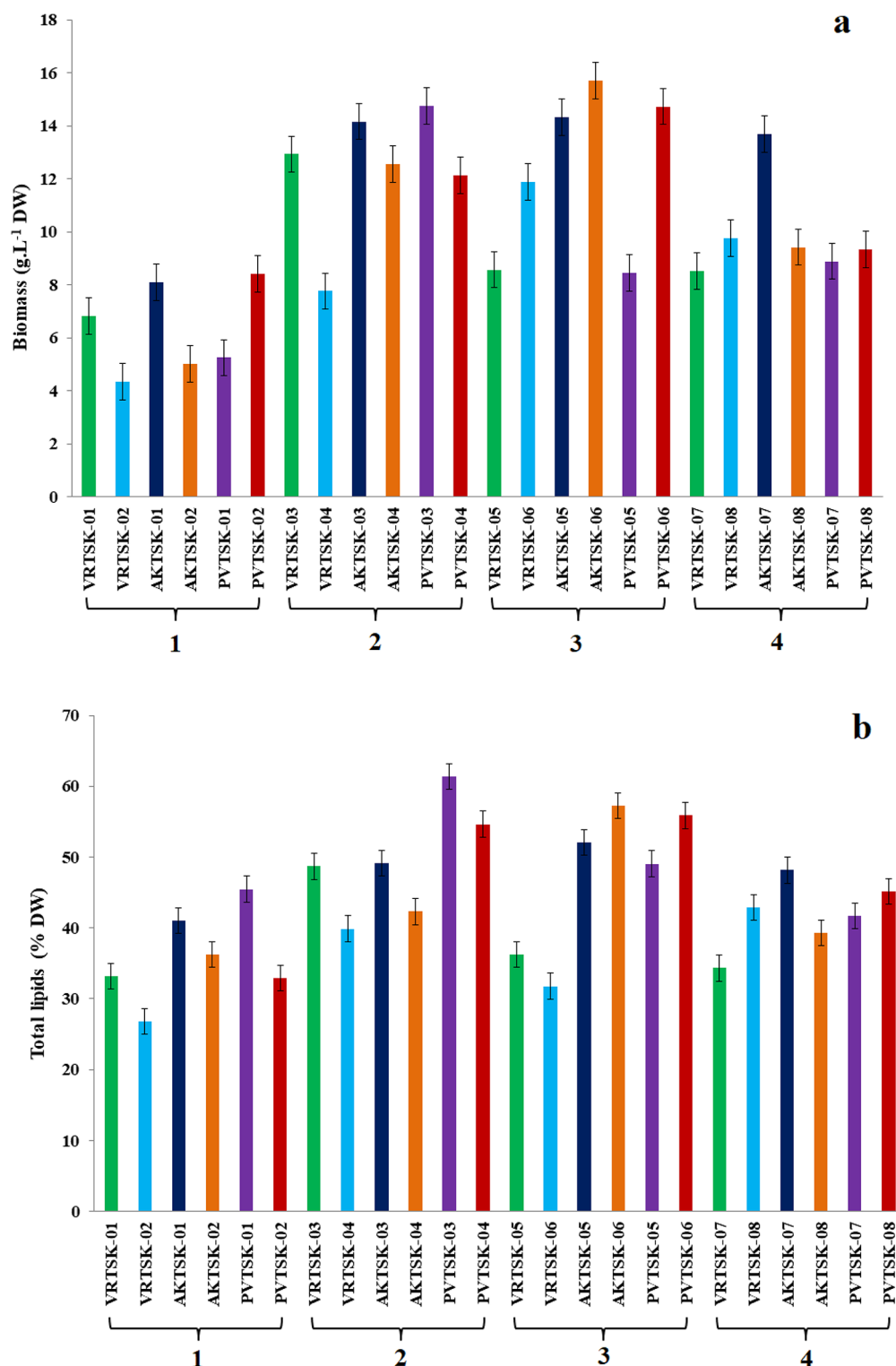


Fig. 10. (a) Biomass and (b) total lipid production of thraustochytrids isolates during different seasons (1. Pre-monsoon, 2. Monsoon, 3. Post-monsoon, 4. Summer).

respectively (Fig. 12a). The most abundant LC-PUFA was DHA (C22:6, n-3), with a relative amount of 23.77–47.46% followed by docosapentaenoic (DPA) (C22:5, n-3) with a relative abundance of 5.83–9.65%. Other LC-PUFAs were eicosapentaenoic acid (EPA) (C20:5, n-3), and arachidonic acid (ARA, C20:4, n-6) with relative abundance of 0.19–9.71% and 0.11–1.28% respectively (Fig. 12b). The strains were found to produce relatively low amount of monounsaturated fatty acids (MUFAs), with Gamma- linolenic acid (C18:3 n-6) ranging from

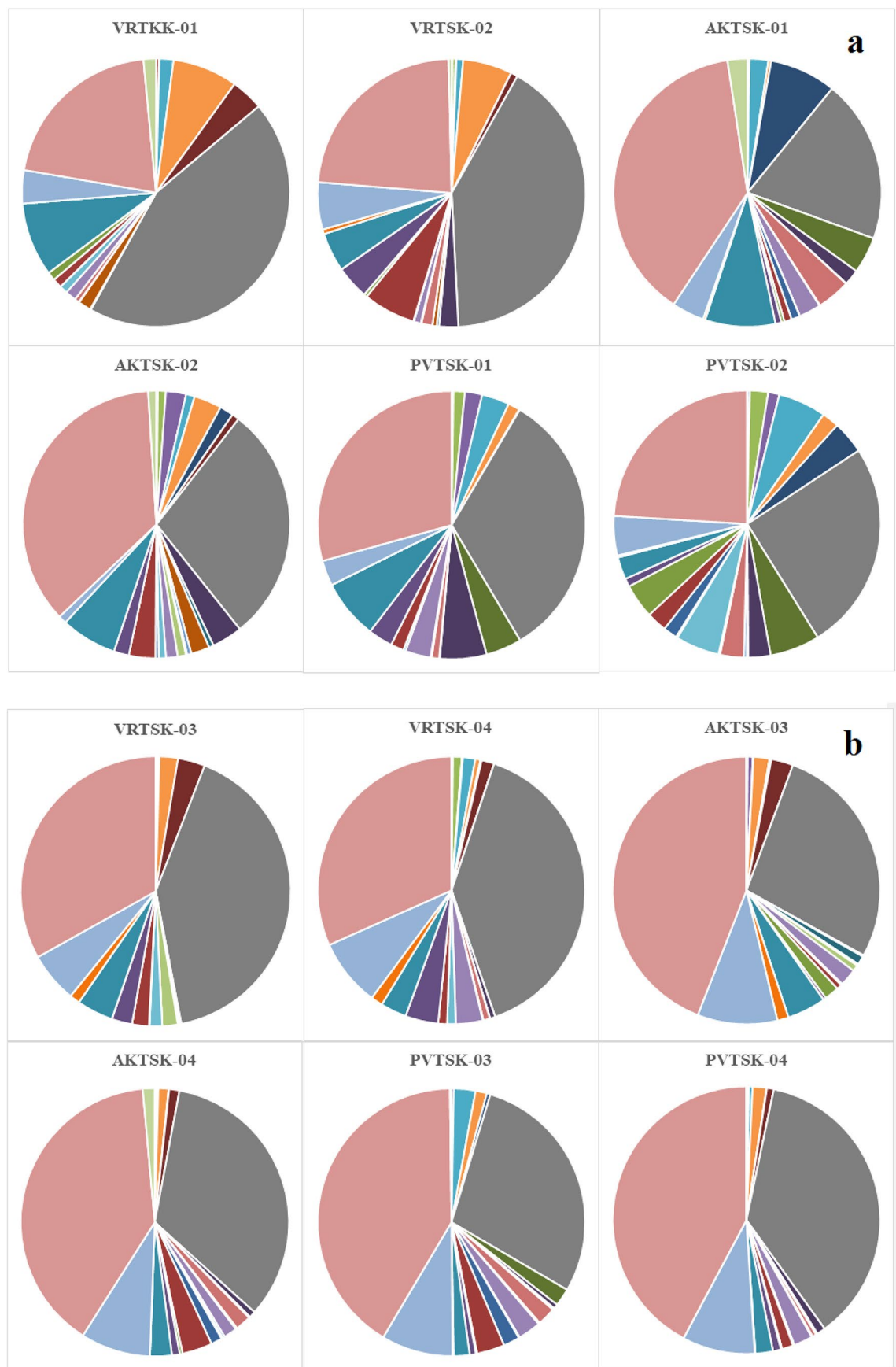


Fig. 11. Fatty acid compositions of thraustochytrid isolates (expressed as % of total fatty acids) during different seasons (**a.** Pre-monsoon, **b.** Monsoon, **c.** Post-monsoon, and **d.** Summer) in Pichavaram, Vellar and Ariyankuppam mangrove habitats.

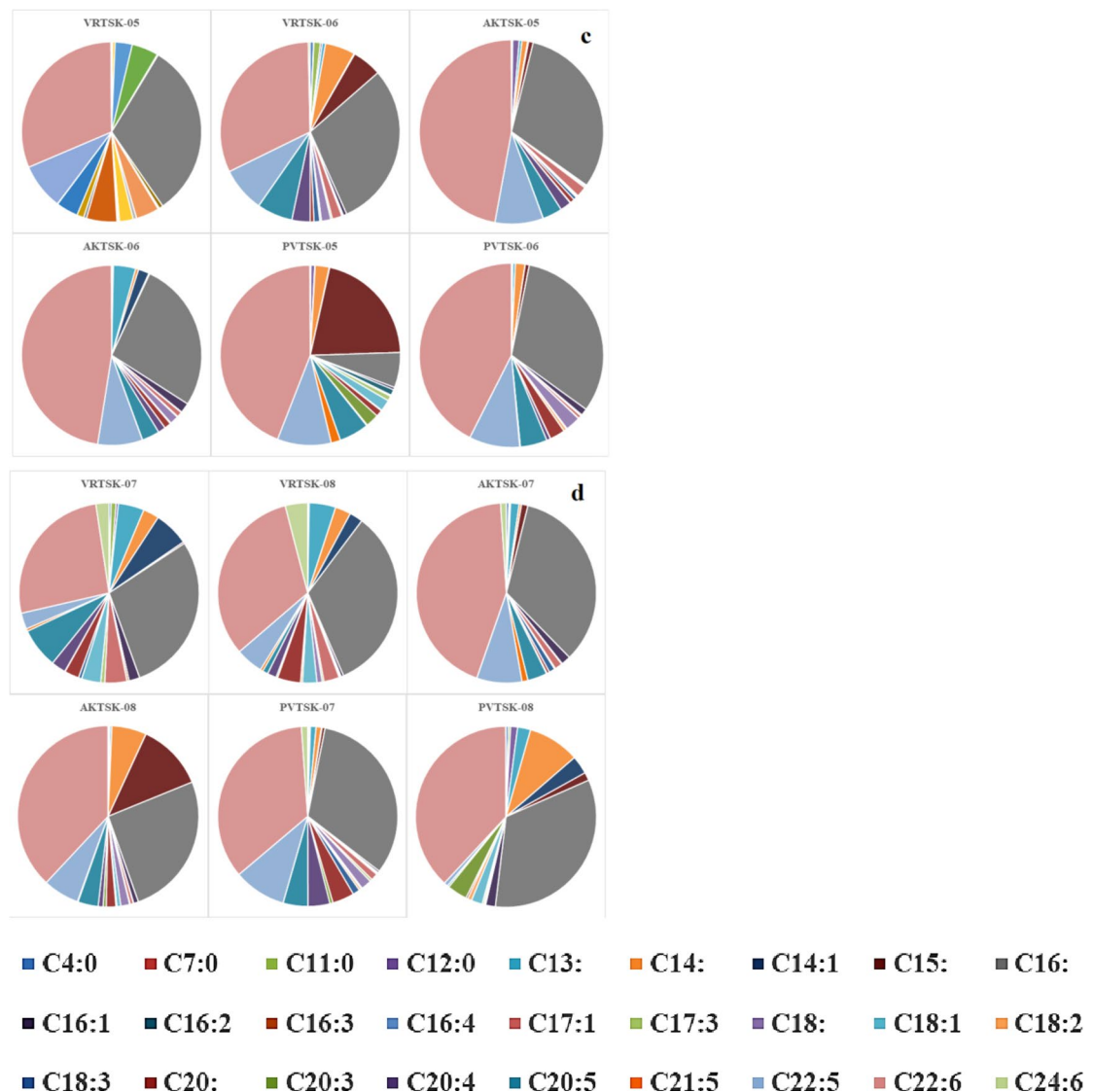


Figure 11. (continued)

0% to 0.72%. The odd chain fatty acids offer several medicinal benefits, including a reduced the risk of type 2 diabetes, cardiovascular disease, and certain forms of cancer^{72,73}.

Seasonal variation of SFAs and PUFAs composition in thraustochytrids is depicted in Fig. 12a and b. SFAs was recorded to be high in pre-monsoon (52.58–60.91%) and post-monsoon (40.78–57.31%), with palmitic acid specifically in the range of 26.15–44.11% and 32.11–40.73%, in those seasons, respectively (Fig. 12a, b, c, and d). Similarly, SFAs was in the range of 42.83–54.91% in monsoon, and 44.50–54.04% in summer with palmitic acid specifically in the range of 27.41–41.06%, and 30.76–44.21% in those seasons respectively. DHA was found to be high in post-monsoon (31.27–47.46%), followed by summer (26.26–43.64%), monsoon (33.59–44.07%), and pre-monsoon (23.77–38.29%) (Fig. 12b). Total PUFA content was high in post-monsoon (42.69–59.22%) and low in pre-monsoon (39.09–47.42%).

DHA is influenced by a number of factors, including water temperature, sunlight, and nutrients. Thraustochytrids from colder places are known to contain more DHA than those from tropical coastal areas. Australian strains have higher DHA content (up to 40%) than Indian strains⁶⁹. However, it is worth noting that the Australian strains have lower biomass production (0.67–3.07 g/L) compared to the Indian strains (7.3–10.6 g/L)¹⁶. In the present study, we recorded the thraustochytrids with high biomass enriched with DHA. It is important to note that the lipids and fatty acids in any organism vary depending on species, season, genetics, and environmental conditions of locations⁷⁴.

Thraustochytrids with high DHA content are shown experimentally to survive in low-temperatures⁶. The cold temperature increases oxidative stress and reduces dissolved oxygen levels, but *Aurantiochytrium* species can maintain cell membrane fluidity which is activated at low temperatures to produce DHA via the polyketide synthase (PKS) metabolic pathway. Therefore, temperature variations lead to the genetic and environmental evolution of various PUFA pathways, such as the PKS pathway in stressful conditions and the traditional fatty

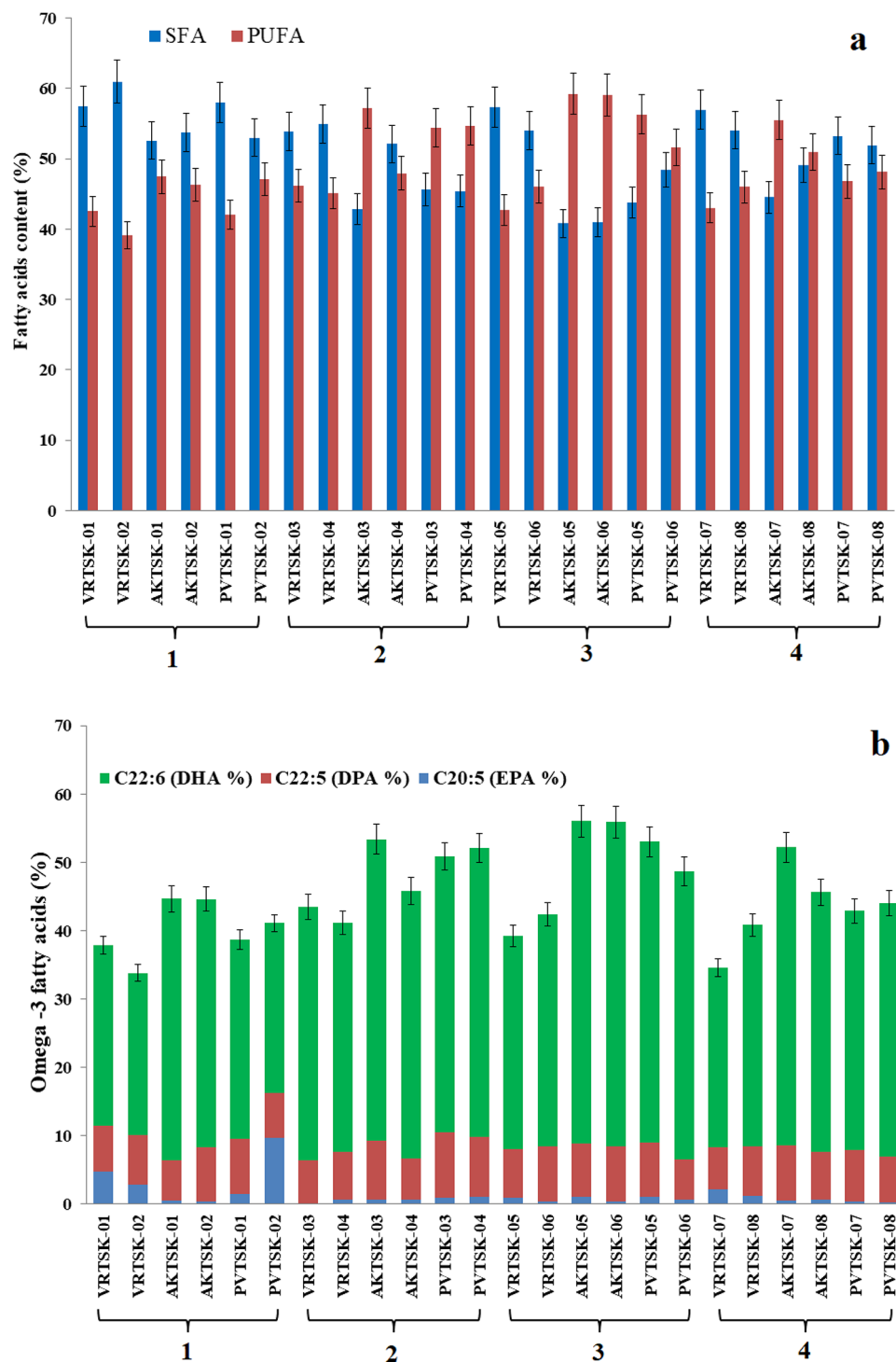


Fig. 12. (a) Fatty acids production of thraustochytrids isolates during different seasons, (b) Seasonal variations of Omega-3 fatty acids context (1. Pre-monsoon, 2. Monsoon, 3. Post-monsoon, 4. Summer).

acid synthase (FAS) pathway under aerobic conditions⁶. Recent transcriptomic studies have shown that under cold conditions, thraustochytrids express many genes involved in the PKS pathway for the synthesis of DHA, DPA, as well as sterols and phosphatidylinositol, which are essential for membrane fluidity^{6,75}.

Carbon and nitrogen play a role in altering the fatty acid composition of thraustochytrids⁷⁰. *Thraustochytrium kinnei* is reported to produce high biomass production of 13.53 g/L, with a total lipid of 41.33% under optimized contents of carbon and nitrogen (Kalidasan et al., 2021a). Similarly, *Aurantiochytrium* ANVKK-06 accumulates high lipid (71.03%) and DHA content of 47.19% of total fatty acids¹⁸. Being a potential source of DHA, thraustochytrids find applications in the nutraceutical, biofuel, and livestock industries². The present

study observed that the thraustochytrid isolates accumulated DHA in a range of 23.77–47.46% during the post-monsoon. Further research is needed to optimize the culture conditions for the growth of thraustochytrids for commercial PUFAs production.

Conclusion

This study investigated thraustochytrids in the root-soil of two mangrove species (*A. marina* and *R. apiculata*) from natural and planted mangrove sites for four different seasons. Thraustochytrid counts were significantly maximum in natural mangroves than in planted mangroves. The count was also maximum in the post-monsoon season than in other seasons. The count exhibited positive correlations with other microbial flora, including lactobacillus, THB, actinobacteria, fungi, *Trichoderma*, azotobacters and yeasts. Similarly, the count of thraustochytrids displayed positive correlations with the presence of N, P, K, Cr, Cu, Mg, Cd, Zn, silt, clay, and redox potential. This suggests that thraustochytrids, in association with other saprophytic microbes, play a role in enriching soil nutrients. Five genera of thraustochytrids, namely *Thraustochytrium*, *Schizochytrium*, *Botryochytrium*, *Parietichytrium*, and *Aurantiochytrium* were identified based on their morphological and molecular features. The study also recorded the highest biomass of 15.71 g/L in *Aurantiochytrium* sp. (AKTSK-06), lipid content of 61.33% in *Aurantiochytrium* sp. (PVTSK-03), and the maximum DHA of 47.46% in *Aurantiochytrium* sp. (AKTSK-06). This study revealed mangroves as an important ecological niche for DHA-rich thraustochytrids. Further studies on the metagenomics of rhizosphere soil will provide more insights into the connections between diverse microbial floras and thraustochytrids in mangrove environments.

Data availability

The datasets used and/or analysed during the current study available from the corresponding author on reasonable request.

Received: 6 June 2024; Accepted: 21 January 2025

Published online: 07 March 2025

References

- Marchan, L. F. et al. Taxonomy, ecology and biotechnological applications of thraustochytrids; A review. *Biotec Advan.* **36**, 26–46. <https://doi.org/10.1016/j.biotechadv.2017.09.003> (2018).
- Wang, Q., Zhang, Y., Hui, R. & Zhu, Y. Marine thraustochytrid: Exploration from taxonomic challenges to biotechnological applications. *Front. Mar. Sci.* **11**, 1371713. <https://doi.org/10.3389/fmars.2024.1371713> (2024).
- Taoka, Y., Nagano, N., Okito, Y. & Izumida, H. Degradation of distillery less (shochu kasu) by cellulose-producing thraustochytrids. *J. Oleo Sci.* **66**, 31–40. <https://doi.org/10.5650/jos.ess16148> (2017).
- Kalidasan, K., Phusit, H. & Kathiresan, K. Enumeration of thraustochytrids in decomposing leaves of mangroves as influenced by physicochemical and microbial factors. *Curr. Res. Environ. Appl. Mycol.* **9**, 288–300. <https://doi.org/10.5943/cream/9/1/24> (2019).
- Bagul, V. P. & Annappure, U. S. Isolation of fast-growing thraustochytrids and seasonal variation on the fatty acid composition of thraustochytrids from mangrove regions of Navi Mumbai, India. *J. Environ. Manag.* **290**, 112597 (2021). <https://doi.org/10.1016/j.jenvman>.
- Paredes, P. et al. Temperature differentially affects gene expression in antarctic thraustochytrid *Oblongichytrium* sp. RT2316-13. *Mar. Drugs* **18**, 563. <https://doi.org/10.3390/md18110563> (2020).
- Wang, Q. et al. Culturable diversity and lipid production profile of Labyrinthulomycete protists isolated from Coastal Mangrove habitats of China. *Mar. Drugs* **17**, 268. <https://doi.org/10.3390/md17050268> (2019).
- Patel, A. et al. Bioprospecting of thraustochytrids for omega-3 fatty acids: A sustainable approach to reduce dependency on animal sources. *Trends Food Sci. Tech.* **115**, 433–444. <https://doi.org/10.1016/j.tifs.2021.06.044> (2021).
- Qu, M., Yeong, H. Y., Pang, K. L. & Phang, S. M. Fatty acid production of tropical thraustochytrids from Malaysian mangroves. *Bot. Mar.* **59**, 321–338. <https://doi.org/10.1515/bot-2016-0031> (2016).
- Saini, R. K., Ravishankar, G. A. & Keum, Y. S. Microalgae and thraustochytrids are sustainable sources of vegan EPA and DHA with commercial feasibility. *Indian J. Microbiol.* <https://doi.org/10.1007/s12088-023-01059-8> (2023).
- Jaritkhuan, S. & Suanjit, S. Species diversity and polyunsaturated fatty acid content of thraustochytrids from fallen mangrove leaves in Chon Buri Province, Thailand. *Agric. Nat. Resour.* **52**, 24–32. <https://doi.org/10.1016/j.anres.2018.05.002> (2018).
- Russo, G. L. et al. Production of omega-3 oil by *Aurantiochytrium mangrovei* using spent osmotic solution from candied fruit industry as sole organic carbon source. *Processes* **9**, 1834. <https://doi.org/10.3390/pr9101834> (2021).
- Chauhan, A. S. et al. Enhanced production of high-value polyunsaturated fatty acids (PUFAs) from potential thraustochytrid *Aurantiochytrium* Sp. *Biore Tech.* **370**, 128536. <https://doi.org/10.1016/j.biortech.2022.128536> (2023).
- Hien, H. T. M. et al. Characterization and optimization of culture conditions for *Aurantiochytrium* sp. SC145 isolated from sand cay (Son ca) island, Vietnam, and antioxidative and neuroprotective activities of its polyunsaturated fatty acids mixture. *Mar. Drugs* **20**, 780. <https://doi.org/10.3390/md20120780> (2022).
- Varada, S. D. Diversity of thraustochytrid protists isolated from brown alga, *Sargassum cinereum* using 18S rDNA sequencing and their morphological response to heavy metals. *J. Mar. Biol. Assoc. UK.* **95**, 265–276. <https://doi.org/10.1017/S0025315414001696> (2015).
- Jaseera, K. V. et al. Isolation and phylogenetic identification of heterotrophic thraustochytrids from mangrove habitats along the southwest coast of India and prospecting their PUFA accumulation. *J. Appl. Phycol.* **31**, 1057–1068. <https://doi.org/10.1007/s10811-018-1627-7> (2018).
- Kalidasan, K., Asmathunisha, N., Gomathi, V., Dufossé, L. & Kathiresan, K. Isolation and optimization of culture conditions of *Thraustochytrium Kinnei* for biomass production, nanoparticle synthesis, antioxidant and antimicrobial activities. *J. Mar. Sci. Eng.* **9**, 678. <https://doi.org/10.3390/jmse9060678> (2021a).
- Kalidasan, K., Vinithkumar, N. V., Peter, D. M., Dharani, G. & Dufossé, L. Thraustochytrids of mangrove habitats from Andaman Islands: Species diversity, PUFA profiles and biotechnological potential. *Mar. Drugs* **19**, 571. <https://doi.org/10.3390/md19100571> (2021b).
- Wang, Q. et al. Enhanced saturated fatty acids accumulation in cultures of newly-isolated strains of *Schizochytrium* sp. and *Thraustochytridae* sp. for large-scale biodiesel production. *Sci. Total Environ.* **631–632** <https://doi.org/10.1016/j.scitotenv.2018.03.078> (2018).
- Raghukumar, S. Thraustochytrid marine protists: Production of PUFAs and other emerging technologies. *Mar. Biotechnol.* **10**, 631–640. <https://doi.org/10.1007/s10126-008-9135-4> (2008).
- Graham, A. et al. Effects of DHA and EPA on cardiovascular indices. *FASEB J.* **35**. <https://doi.org/10.1096/fasebj> (2021).

22. Wakeel, S. K. E. & Riley, J. P. The determination of organic carbon in marine muds. *J. De Conseil Permanent Intl Pour l Explor. de la Mer.* **22**, 180–183 (1956).
23. Subbiah, B. V. & Asija, G. L. A rapid procedure for the determination of available nitrogen in soils. *Curr. Sci.* **31**, 196–200 (1956).
24. Guzman, H. M. & Jimenez, C. E. Contamination of coral reefs by heavy metals along the Caribbean coast of Central America (Costa Rica and Panama). *Mar. Pollut. Bull.* **24**, 554–561. [https://doi.org/10.1016/0025-326X\(92\)90708-E](https://doi.org/10.1016/0025-326X(92)90708-E) (1992).
25. Chester, R. & Hughes, F. G. A chemical technique for the separation of ferro manganese minerals, carbonate minerals and absorbed trace elements from pelagic sediment. *Chem. Geol.* **2**, 249–262. [https://doi.org/10.1016/0009-2541\(67\)90025-3](https://doi.org/10.1016/0009-2541(67)90025-3) (1967).
26. Gawas, V. S. et al. Diversity and extracellular enzyme activities of heterotrophic bacteria from sediments of the Central Indian Ocean Basin. *Sci. Rep.* **28**, 9403. <https://doi.org/10.1038/s41598-019-45792-x> (2019).
27. Waterbury, J. B. & Stanier, R. Y. Isolation and growth of cyanobacteria from marine and hypersaline environments. In: (eds Starr, M. P., Stolp, H., Trüper, H. G., Balows, A. & Schlegel, H. G.) *The Prokaryotes*. https://doi.org/10.1007/978-3-662-13187-9_9 (Springer, 1981).
28. Thiruneelakandan, G., Sesuraj, V. J., Babu, V. & Senthil Kumar, V. Efficacy of preserving sea foods using marine *Lactobacillus*. *Sci. Technol. Arts Res. J.* **2**, 10–13. <https://doi.org/10.4314/star.v2i4.3> (2013).
29. Ambikapathy, V., Babu, S., Anbukumar, A., Shijila Rani, A. S. & Prakash, P. Isolation of actinobacteria from mangrove plants. In *Methods in Actinobacteriology. Springer Protocols Handbooks* (Dharumadurai, D. eds.). (Humana, 2022). <https://doi.org/10.1007/978-1-0716-1728-1-13>
30. Sandeep, U., Narendra, K., Sing, V. K. & Anshuman, S. Isolation, characterization, and morphological study of *Azotobacter* isolates. *J. Appl. Nat. Sci.* **7**, 984–990. <https://doi.org/10.31018/jans.v7i2.718> (2015).
31. Fell, J. W. The role of nucleotide analysis in the systematics of the yeast genera *Cryptococcus* sp. and *Rhodotorula* sp. *Stud. Mycol.* **38**, 129–146 (2005).
32. Askew, D. J. & Laing, M. D. An adapted selective medium for the quantitative isolation of *Trichoderma* Sp. *Plan. Pathol.* **42**, 686–690. <https://doi.org/10.1111/j.1365-3059.1993> (1993).
33. Ravikumar, K., Venkatesh, K. S. & Umesh-Kumar, S. Evidence that cleavage of the precursor enzyme by autocatalysis secretion of multiple amylases by *Aspergillus niger*. *FEBS Lett.* **557**, 239–242. [https://doi.org/10.1016/S0014-5793\(03\)01510-2](https://doi.org/10.1016/S0014-5793(03)01510-2) (2004b).
34. Koopmann, I. K., Müller, B. A. & Labes, A. Screening of a thraustochytrid strain collection for carotenoid and squalene production characterized by cluster analysis, comparison of 18S rRNA gene sequences, growth behavior, and morphology. *Mar. Drug.* **21**, 204. <https://doi.org/10.3390/md21040204> (2023).
35. Kalidasan, K. et al. PUFA and carotenoid producing thraustochytrids and their anti-microbial and antioxidant activities. *Front. Mar. Sci.* **10**, 1126452. <https://doi.org/10.3389/fmars.2023.1126452> (2023).
36. Folch, J., Lees, M. & Stanley, G. H. A simple method for the isolation and purification of the total lipids from animal tissues. *J. Biol. Chem.* **226**, 497–509. [https://doi.org/10.1016/S0021-9258\(18\)64849-5](https://doi.org/10.1016/S0021-9258(18)64849-5) (1957).
37. Kashiwagi, T., Meyer-Rochow, V. B., Nishimura, K. & Eguchi, E. Fatty acid composition and ultrastructure of photoreceptive membranes in the crayfish *Procambarus clarkii* under conditions of thermal and photic stress. *J. Comp. Physiol.* **167**, 1–8. <https://doi.org/10.1007/s003600050041> (1997).
38. Kathiresan, K. & Ravikumar, S. Influence of tannins, sugars, and amino acids on bacterial load of marine halophytes. *Environ. Ecol.* **13**, 94–96 (1995a).
39. Danielson, R. M. & Davey, C. B. Non-nutritional factors affecting the growth of *Trichoderma* in culture. *Soil. Biol. Biochem.* **5**, 495–504. [https://doi.org/10.1016/0038-0717\(73\)90039-4](https://doi.org/10.1016/0038-0717(73)90039-4) (1973).
40. Rajendran, N. & Kathiresan, K. Microbial flora associated with submerged mangrove leaf litter in India. *Rev. Biol. Trop.* **55**, 393–400. <https://doi.org/10.15517/rbt.v55i2.6019> (2007).
41. Saravanakumar, K. et al. Soil-microbial communities indexing from mangroves rhizosphere and barren sandy habitats. *Physiol. Mol. Plant. Pathol.* **104**, 58–68. <https://doi.org/10.1016/j.pmp.2018.09.005> (2018).
42. Alvarenga, D. O., Rigonato, J., Branco, L. H. Z. & Fiore, M. F. Cyanobacteria in mangrove ecosystems. *Biodivers. Conserv.* **24**, 799–817. <https://doi.org/10.1007/s10531-015-0871-2> (2015).
43. Nabeel, M. A. et al. Contribution by microbes to the food web of a mangrove biotope: The approach of carbon and nitrogen stable isotopes. *Afr. J. Mar. Sci.* **32**, 65–70 (2010).
44. Kathiresan, K. & Thiruneelakandan, G. Prospects of lactic acid bacteria of marine origin. *Ind. J. Biotech.* **7**, 170–177 (2008).
45. Noraphat, H., Chobert, J. M. & Kittikun, A. H. Bacteriocin-producing lactic acid bacteria isolated from mangrove forests in southern Thailand as potential bio-control agents in food: Isolation, screening, and optimization. *Food Control* **41**, 202–211. <https://doi.org/10.1016/j.foodcont.2014.01.021> (2014).
46. Shome, R., Shome, B. R., Mandal, A. B. & Bandopadhyay, A. K. Bacterial flora in mangroves of Andaman - part I: Isolation, identification and antibiogram studies. *Ind. J. Mar. Sci.* **24**, 97–98 (1995).
47. Shiao, Y. J. et al. Composition and activity of N₂-fixing microorganisms in mangrove forest soils. *Forests* **12**, 822. <https://doi.org/10.3390/f12070822> (2021).
48. Saravanakumar, K., Anburaj, R., Gomathi, V. & Kathiresan, K. Ecology of soil microbes in a tropical mangrove forest of southeast coast of India. *Biocatal. Agric. Biotechnol.* **8**, 73–85. <https://doi.org/10.1016/j.bcab.2016.08.010> (2016).
49. Manivasagan, P. et al. Marine actinobacteria: An important source of bioactive natural products. *Environ. Toxicol. Pharmacol.* **38**, 172–188. <https://doi.org/10.1016/j.etap.2014.05.014> (2014).
50. Kaewkrajay, C., Channmethakul, T. & Limtong, S. Assessment of diversity of culturable marine yeasts associated with corals and zoanthids in the gulf of Thailand, south China Sea. *Microorgan* **26**, 474. <https://doi.org/10.3390/microorganisms8040474> (2020).
51. Zhu, H. Y. et al. Diversity and distribution of yeasts in intertidal zones of China. *Front. Mar. Sci.* 1286511. <https://doi.org/10.3389/fmars.2023> (2023).
52. Chi, Z. M., Liu, T. T., Chi, Z., Liu, G. L. & Wang, Z. P. Occurrence and diversity of yeasts in the mangrove ecosystems in Fujian, Guangdong and Hainan provinces of China. *Ind. J. Microbiol.* **52**, 346–353. <https://doi.org/10.1007/s12088-012-0251-5> (2012).
53. Ding, M. Y. et al. Emerging salt marshes as a source of *Trichoderma arenarium* sp. nov. and other fungal bioeffectors for biosaline agriculture. *J. Appl. Microbiol.* **130**, 179–195. <https://doi.org/10.1111/jam.14751> (2020).
54. Saravanakumar, K., Arasu, S., Kathiresan, K. & V., & Effect of *Trichoderma* on soil phosphate solubilization and growth improvement of *Avicennia marina*. *Aquat. Bot.* **104**, 101–105. <https://doi.org/10.1016/j.aquabot.2012.09.001> (2013).
55. Narendran, R., Kathiresan, K., Sathishkumar, R. S., Kayalvizhi, K. & Sundaramanickam, A. Bioremoval of toxic substances in synthetic wastewater using *Trichoderma pubescens* (NPK2), isolated from mangrove soil. **19**, 101100 (2019). <https://doi.org/10.1016/j.bcab.2019>
56. Liu, M., Huang, H., Bao, S. & Tong, Y. Microbial community structure of soils in Bamenwan mangrove wetland. *Sci. Rep.* **9**, 8406. <https://doi.org/10.1038/s41598-019-44788-x> (2019).
57. Jones, E. B. G. & Harrison, J. L. Physiology of marine phycocyanocystes. In *Recent Advances in Aquatic Mycology* (E.B. Gareth Jones, ed.). 261–277 (Elek Science, 1976).
58. Dewiyanthi, D., Darmawati, Z. A., Muchlisin, T. Z., Helmi, I., Defira, C. N. & Imelda, & Physical and chemical characteristics of soil in mangrove ecosystem based on differences habitat in Banda Aceh and Aceh Besar. *IOP Conf. Ser. Earth Environ. Sci.* 674012092. <https://doi.org/10.1088/1755-1315/674/1/012092> (2021).
59. Kamal, A. H. M. et al. A. Nutrient properties of tidal-borne alluvial sediments from a tropical mangrove ecosystem. *Reg. Stud. Mar. Sci.* **36**, 101299. <https://doi.org/10.1016/j.rsma.2020> (2020).

60. Jimenez, L. C. Z., Queiroz, H. M., Otero, X. L., Nóbrega, G. N. & Ferreira, T. O. Soil organic matter responses to mangrove restoration: A replanting experience in Northeast Brazil. *Int. J. Environ. Res. Public. Health* **18**, 898. <https://doi.org/10.3390/ijerph18178981> (2021).
61. Xue, B., Yan, C. L., Lu, H. L. & Bai, Y. Mangrove-derived organic carbon in sediment from Zhangjiang estuary (China) mangrove wetland. *J. Coast Res.* **25**, 949–956. <https://doi.org/10.2112/08-1047.1> (2009).
62. Kathiresan, K., Gomathi, V., Anburaj, R. & Saravanakumar, K. Impact of mangrove vegetation on seasonal carbon burial and other sediment characteristics in the Vellar-Coleroon Estuary, India. *J. For. Res.* **25**, 787–794. <https://doi.org/10.1007/s11676-014-0526-2> (2014).
63. Kristensen, E., Bouillon, S., Dittmar, T. & Marchand, C. Organic carbon dynamics in mangrove ecosystems: A review. *Aquat. Bot.* **89**, 201–219. <https://doi.org/10.1016/j.aquabot.2007.12.005> (2008).
64. Wu, H. et al. Unveiling the crucial role of soil microorganisms in carbon cycling. *Review* **909**, 168627. <https://doi.org/10.1016/j.scitotenv.2023.168627> (2024).
65. Islam, M. A. et al. Microbiota and soil fauna mediate litter decomposition and associated carbon and nitrogen dynamics in mangrove blue carbon ecosystems: insights from a coastal lagoon in Malaysia. *Hydrobiologia* <https://doi.org/10.1007/s10750-024-05470-0> (2023).
66. Pang, K. L. et al. Cu (II) pollution affects fecundity of the mangrove degrader community, the labyrinthulomycetes. *Bot. Mar.* **58**, 129–138. <https://doi.org/10.1515/bot-2015-0006> (2015).
67. Dellero, Y. et al. Proposal of a new thraustochytrid genus *Hondaia* gen. nov. and comparison of its lipid dynamics with the closely related pseudo-cryptic genus *Aurantiochytrium*. *Algal Res.* **35**, 125–141 (2018). <https://doi.org/10.1016/j.algal.2018.08.018>
68. Liu, Y., Singh, P., Sun, Y., Luan, S., & Wang, G. Culturable diversity and biochemical features of thraustochytrids from coastal waters of Southern China. *Appl. Microbiol. Biotechnol.* **98**, 3241–55. <https://doi.org/10.1007/s00253-013-5391-y> (2014).
69. Gupta, A. et al. Exploring omega-3 fatty acids, enzymes and biodiesel producing thraustochytrids from Australian and Indian marine biodiversity. *Biotech J* **11**, 345–355. <https://doi.org/10.1002/biot.201500279> (2016).
70. Pawar, P. R., Velani, S., Kumari, S., Lali, A. M. & Prakash, G. Isolation, and optimization of a novel thraustochytrid strain for DHA rich and astaxanthin comprising biomass as aquafeed supplement. *Biotech* **11**, 71. <https://doi.org/10.1007/s13205-020-02616-4> (2021).
71. Aini, U. N., Lunprom, S., Reungsang, A. & Salakkam, A. Docosahexaenoic acid (DHA) production by *Aurantiochytrium limacinum* using cassava pulp hydrolysate as an alternative low-cost carbon source. *Front. Mar. Sci.* **9** (2022). <https://doi.org/10.3389/fmars.985119> (2022).
72. Jenkins, B., West, J. A. & Koulman, A. A review of odd-chain fatty acid metabolism and the role of pentadecanoic acid (C15:0) and heptadecanoic acid (C17:0) in health and disease. *Molecules* **20**, 2425–2444. <https://doi.org/10.3390/molecules20022425> (2015).
73. Venn-Watson, S., Lumpkin, R. & Dennis, E. A. Efficacy of dietary odd-chain saturated fatty acid pentadecanoic acid parallels broad associated health benefits in humans: Could it be essential? *Sci. Rep.* **10**, 8161. <https://doi.org/10.1038/s41598-020-64960-y> (2020).
74. Polat, S. & Ozgul, Y. Seasonal proximate and fatty acid variations of some seaweeds from the Northeastern Mediterranean Coast. *Oceanologia* **55**, 375–391. <https://doi.org/10.5697/oc.55-2.375> (2013).
75. Ma, Z. et al. Transcriptome and gene expression analysis of DHA producer *Aurantiochytrium* under low temperature conditions. *Sci. Rep.* **5**, 1–13. <https://doi.org/10.1038/srep14446> (2015).

Acknowledgements

The authors are thankful to Second Century Fund (C2F) for postdoctoral fellowship and to the authorities of Chulalongkorn University, Thailand.

Author contributions

Kal K designed the study, performed the laboratory experiments, prepared the draft, performed the data analysis, and completed the writing – review & editing of the manuscript. VV, and SC designed the study, supervised the work, reviewed, edited, and approved the manuscript. NK, reviewed and edited the manuscript. Kat K, and NVV helped to design the study, reviewed, and edited the manuscript. All authors contributed to the article and approved the submitted version.

Funding

The authors are thankful to Thailand Science Research and Innovation Fund Chulalongkorn University (4710411), the Second Century Fund (C2F) for the postdoctoral fellowship, Thailand Science Research and Innovation Fund Chulalongkorn University (DIS66230010), and Science and Engineering Research Board (SERB), New Delhi, India under the National Postdoctoral Fellowship, PDF/2017/002579.

Declarations

Competing interests

The authors declare no competing interests.

Additional information

Correspondence and requests for materials should be addressed to K.K. or V.V.

Reprints and permissions information is available at www.nature.com/reprints.

Publisher's note Springer Nature remains neutral with regard to jurisdictional claims in published maps and institutional affiliations.

Open Access This article is licensed under a Creative Commons Attribution-NonCommercial-NoDerivatives 4.0 International License, which permits any non-commercial use, sharing, distribution and reproduction in any medium or format, as long as you give appropriate credit to the original author(s) and the source, provide a link to the Creative Commons licence, and indicate if you modified the licensed material. You do not have permission under this licence to share adapted material derived from this article or parts of it. The images or other third party material in this article are included in the article's Creative Commons licence, unless indicated otherwise in a credit line to the material. If material is not included in the article's Creative Commons licence and your intended use is not permitted by statutory regulation or exceeds the permitted use, you will need to obtain permission directly from the copyright holder. To view a copy of this licence, visit <http://creativecommons.org/licenses/by-nc-nd/4.0/>.

© The Author(s) 2025